
Algebraic Machine Learning for Small-to-Medium Datasets Is Competitive against Strong Standard Baselines

David Méndez

Mathematics of Behavior and Intelligence Lab
Champalimaud Foundation, Lisbon
david.mendez@research.fchampalimaud.org

Fernando Martin-Maroto

Mathematics of Behavior and Intelligence Lab
Champalimaud Foundation, Lisbon
fernando.martinmaroto@neuro.fchampalimaud.org

Gonzalo G. de Polavieja

Mathematics of Behavior and Intelligence Lab
Champalimaud Foundation, Lisbon
gonzalo.polavieja@neuro.fchampalimaud.org

Abstract

Symbolic methods are generally not considered competitive with strong modern learners on realistic supervised tasks. We evaluate Algebraic Machine Learning (AML), a framework that learns through subdirect decomposition of algebraic structure rather than numerical optimization, against standard baselines on image and tabular classification across varying training-set sizes. We find that AML trained only on training data without using validation or cross-validation outperforms a family of cross-validated baseline methods including CNNs on small to medium image datasets (50–2000 training examples). On tabular datasets in the same size range, XGBoost is overall the best performing method, but AML is nonetheless comparable to methods incorporating task-specific biases such as LightGBM and random forests. AML achieves this competitive performance across two very different types of datasets using a generic algebraic inductive bias, rather than the modality-specific biases built into standard baselines like CNNs for images or XGBoost for tabular data, and requires no cross validation because it has no task-dependent hyperparameters to tune.

1 Introduction

Supervised learning is usually formulated as numerical optimization over a parameterized model class. In this paradigm, inductive bias is encoded through model architecture, regularization, kernels, or ensemble structure, and performance is often determined not only by the learner but also by hyperparameter selection and validation protocol. This view underlies much of modern machine learning, including neural networks, boosted trees, random forests, and support vector machines [1, 2, 3, 4, 5].

Symbolic approaches to artificial intelligence follow a different tradition. Classical systems represented knowledge explicitly, typically through rules, logical relations, or expert-curated struc-

tures [6, 7, 8]. These systems were successful in domains where knowledge could be formalized, but they depended heavily on expert input and were difficult to maintain or scale. As data became abundant and computational resources improved, the field largely shifted away from symbolic learning toward statistical and parametric methods, and symbolic methods are now in common use mainly in niche scenarios involving explicit reasoning or knowledge representation. A common working assumption is that symbolic methods are not competitive on realistic supervised learning tasks unless they are combined with, or subordinated to, modern numerical learners.

This paper tests that assumption. We study *Algebraic Machine Learning* (AML) [9, 10, 11], a symbolic learning framework in which models are constructed through subdirect decomposition (a way of breaking an algebra into irreducible components; see §3), rather than through gradient-based or combinatorial optimization of a parameterized objective. AML can incorporate manually specified symbolic relations, but it can also learn directly from data. This makes it possible to evaluate AML not as an expert system, but as a supervised learner.

We focus on classification tasks in two distinct modalities: images and tabular data. Inputs are encoded symbolically from their component features, and the only manually supplied formal knowledge is the order relation between numerical feature values. We provide the necessary background on the algebraic encoding and learning procedure in §3; the full algebraic framework, theoretical foundations, and the main learning algorithm, Sparse Crossing, are developed in [9, 10, 11].

Our experimental question is whether a generic algebraic inductive bias can compete with standard supervised baselines that use modality-specific biases and cross-validated hyperparameters. To answer this, we compare a single AML run, trained only on the training set, against cross-validated baseline families. The baselines include convolutional neural networks for image classification and boosted-tree methods for tabular classification, giving the standard methods the advantage of task-specific architecture and validation-based model selection. A practical consequence of AML’s design is that it does not require a held-out validation set as it does not have task-dependent hyperparameters to tune, which is particularly relevant in low-data regimes where every labeled example is scarce.

Our contributions are as follows:

1. We provide a systematic empirical evaluation of AML on supervised image and tabular classification across training-set sizes from 50 to 2000 examples.
2. We compare AML against strong cross-validated baselines, including CNNs for images and XGBoost, LightGBM, and random forests for tabular data.
3. We show that AML is highly competitive in low- and medium-data regimes despite using a generic algebraic inductive bias and no task-dependent hyperparameter tuning.

Across twelve standard image datasets, AML with a logistic regression readout is the best-performing method in aggregate over the evaluated training sizes, statistically distinguishable from each baseline; it is also the best-performing method on a plurality of datasets in the 200–1000 example range. Across 29 tabular datasets, AML is not the strongest method overall: XGBoost performs best in aggregate, and is the only baseline statistically distinguishable from AML. AML is otherwise comparable to strong tabular baselines such as LightGBM and random forests, and achieves the best result on a plurality of datasets at 1000 training examples. These findings suggest that symbolic learning can be competitive in realistic supervised tasks when the symbolic structure is learned from data rather than manually engineered.

2 Related Work

Parameterized learners. CNNs encode locality and translation equivariance for vision [12]. Boosted-tree methods provide strong priors through additive recursive partitioning [3, 13]. Random forests favor ensembles of shallow trees [4]. SVMs favor large-margin separation [5]. These methods have been the standard tools for supervised classification across the modalities we study, and they share two relevant properties: their inductive biases are tailored to specific input modalities, and their performance depends on hyperparameter selection via cross-validation. We use them as the baselines against which to compare AML’s design, which is modality-agnostic and requires no task-dependent hyperparameter tuning.

Low-data and few-shot methods. Meta-learning [14], transfer from pretrained representations [15], and data augmentation address low-data settings by importing external structure. We deliberately exclude these from our comparison: our question is whether algebraic learning is competitive with standard supervised baselines trained from scratch, not whether it beats methods that leverage auxiliary data.

Classical and neurosymbolic AI. Classical symbolic AI represents knowledge through rules and logic [6, 7, 8]. Neurosymbolic systems [16, 17] combine symbolic constraints with neural learners, typically using symbolic components to guide or regularize an underlying neural model. AML differs from both: its algebraic structure is learned from data (unlike classical systems) and *is* the model itself (unlike most neurosymbolic approaches).

Algebra in machine learning. Algebraic ideas appear in equivariant networks [18], algebraic statistics [19], and category-theoretic frameworks [20]. In these settings algebra describes model classes or invariances. AML differs in that subdirect decomposition is itself the learning mechanism.

AML foundations. The algebraic framework, including mathematical rule recovery guarantees, generalization analysis, and Sparse Crossing algorithm, was developed in [9, 10, 11]. A more in-depth introduction to the computational and statistical aspects of learning in AML can be found in [21]. The present paper does not modify the AML framework; we use it as developed in this prior work and focus instead on a systematic empirical evaluation against modern baselines.

3 Background: Algebraic Machine Learning

We summarize the AML framework developed in [9, 10, 11]; the reader is referred to those papers for formal definitions, proofs, and algorithmic details.

In AML, rules and data are encoded as relationships between elements in an algebra, where the word algebra is used as in the language of Universal Algebra. Namely, an algebra is a set A together with one or several operations $f : A^n \rightarrow A$ [22]. The algebras used in this framework are *semilattices*, where a semilattice is an algebra A with a single binary operation $\odot : A \times A \rightarrow A$, which must additionally be commutative ($a \odot b = b \odot a$), associative ($a \odot (b \odot c) = (a \odot b) \odot c$) and idempotent ($a \odot a = a$) [23]. Every semilattice carries a natural partial order: $a \leq b$ if and only if $b = a \odot b$, written equivalently as a is in b . We use this order relation as the central object throughout learning.

3.1 Encoding a classification problem into the algebras

Tasks are encoded in this framework by building semilattices tailored to the task at hand. We consider a set C of *constants*, which are the basic symbols used to represent the data and rules we need to encode a task (a grayscale intensity at a pixel, a value of a categorical or numerical variable, a label in a classification task). A data-point is encoded as the product \odot of all constants representing its features; we call any such product a *term*.

For example, a grayscale image is encoded by constants $c_{i,j,s}$, one per pixel position (i, j) and intensity s , and its term is the product $\odot_{i,j} c_{i,j,s(i,j)}$, where $s(i, j)$ is the intensity at (i, j) . Tabular data-points are encoded analogously, with one constant per (variable, value) pair; missing values are handled by simply omitting the corresponding constants from the term.

In the learning process, we start with an algebra with no relations between constants, the *freest semilattice*. After training, we obtain an algebra in which each example’s term t satisfies $c_{l_i} \leq t$ for its true label l_i ((c_{l_i}, t) is a *positive duple*) and $c_{l_j} \not\leq t$ for any other label l_j ((c_{l_j}, t) is a *negative duple*), where c_l is the constant encoding the label l . Order relations between numerical-variable values are encoded similarly via order between their constants; we use two oppositely-ordered chains per numerical variable to capture both ascending and descending information [21]. No other formal knowledge is supplied to the system in this paper.

3.2 Learning by subdirect decomposition

Every algebra admits a subdirect decomposition into irreducible components [24]. AML tracks this decomposition computationally via *atoms*: elements determined by subsets of constants in C that,

collectively, determine the order relation in the algebra and correspond bijectively to the irreducible components of a subdirect decomposition of the algebra [10, Theorem 37]. An atom ϕ discriminates a duple t_1, t_2 if $\phi < t_1$ (one of the constants that determine ϕ is in t_1) and $\phi \not< t_2$. The inequality $t_1 \leq t_2$ holds in the algebra if and only if no atoms discriminate (t_1, t_2) .

Learning in AML is thus reduced to finding an atomization satisfying the duples that encode the task: no atom discriminates the positive duples, and at least one atom discriminates each negative duple. The Sparse Crossing algorithm [9] performs this construction iteratively. Given a current atomization and a batch of duples, it removes atoms discriminating the positive duples and adds atoms to discriminate the negative duples, in a way that generalizes to unseen data.

3.3 The computational learning pipeline

Our learning pipeline mostly follows that of [21], where it is explained in more detail; we modified the batch sizes to match our smaller number of train examples. In short, we start with the freest semilattice and successively use sparse crossing to enforce batches of duples. In each batch, sparse crossing produces a new model, the *master model*; as well as a model that aggregates information across batches, the *union model*.

We train (i.e., perform sparse crossing) for a maximum of 1000 batches. We start with batches consisting of 1/3 of all positive and negative example-related duples, and linearly grow the batch size until each batch contains all of the task’s duples after 666 batches, or 2/3 of the maximum number of batches. Duples encoding the order of numerical variables are always enforced. We stop training early if the union model perfectly encodes the entire train dataset for 40 consecutive batches.

After training, we reduce the union model to 10% of its size. We do so in such a way that all atoms are individually discriminative of at least one negative example, collectively discriminate all negative duples in the training set, and are diverse in the duples they discriminate. This both promotes generalization and reduces inference cost. We do so in a loop of independent computations, in each of which, we randomly sort the negative duples, and beginning from an empty set of atoms S , for each duple r , we test if there is already a duple in S discriminating r and, if not, randomly sample atoms from the union model until one discriminates r and add it to S . We perform this iteratively until the union of all of these subsets reaches the desired size.

For test-time evaluation, we cannot directly check which positive duples hold in the model as there are usually examples for which all duples tied to classification are discriminated by some atom. In [21] the authors classify in AML in two ways. The first way uses the algebraic information directly: they classify an example as belonging to the class for which the corresponding classification duple is discriminated by the fewest number of atoms, which they call *fewest misses*. The second way uses a *logistic regression readout* on the atomization, thus weighing atoms by their statistical importance for classification. We elected to use the logistic regression readout for our headline results (§5.1 and §5.2) as they consistently produce stronger F_1 scores, but we nonetheless evaluate the fewest misses variant in §5.3 to characterize how much of AML’s competitiveness depends on the readout versus the algebraic atomization itself.

In the logistic regression readout, each example produces a ± 1 vector indexed by atoms (entry +1 if the atom is below the example’s term, -1 otherwise), and a single fully-connected linear layer is trained on top to predict the class. This readout is trained on the same training data used for the algebra until the per-example average train loss falls below 10^{-7} ; no validation data is used at any step.

4 Experimental Setup

The same encoding framework is used for both modalities for AML, as per §3: constants represent primitive feature–value pairs and class labels, and examples are encoded as terms. No modality-specific structure (e.g. spatial adjacency for pixels, feature interactions for tabular data) is introduced.

Images. Due to AML’s computational cost on high-resolution inputs, we restrict to eleven datasets at 32×32 or lower resolution, plus COIL-20 at 128×128 . The selection covers handwriting recognition (MNIST [25], Kuzushiji-49 [26]), medical imaging (BloodMNIST [27], OrganCMNIST [28], PneumoniaMNIST [29], DermaMNIST [30, 31], part of MedMNIST [32]) and general object recog-

inition (CIFAR-10 [33], Fashion-MNIST [34], STL-10 [35], Aerial Cactus Identification [36, 37], Street View House Number [38], COIL-20 [39]). Datasets span 2–49 classes, and include both grayscale and color images. STL-10 is down-scaled to 32×32 as per [35]; all other datasets are presented at native resolution. We use each dataset’s provided train/test split where available; for COIL-20, which has no canonical split, we randomly hold out 22 images per object (440 total) for the test set. Both AML and the baselines receive identical training and test data: the first n training examples (after shuffling, for COIL-20) are used for each $n \in \{50, 100, 200, 500, 1000, 2000\}$ (no $n = 2000$ for COIL-20). Dataset characteristics are detailed in Appendix A, Table 3.

Tabular data. We use the 29 tabular datasets selected for primary evaluation of classification tasks in [40], which span 2–308 features (mixed categorical and numerical) and 2–10 classes. These datasets do not come with pre-defined splits, so we randomly hold out 10% of each dataset for testing. For each $n \in \{50, 100, 200, 500, 1000, 2000\}$, the first n examples (after shuffling) of the remaining data form the training set, ensuring AML and baselines see identical data. Dataset characteristics are in Appendix A, Table 4.

4.1 Baselines

All baselines use cross-validated hyperparameter selection. AML uses fixed hyperparameters, with no dataset-specific tuning and no validation data. These parameters include those already introduced in §3.3, and other hyperparameters discussed in [21], see Appendix B.2.

Our baselines comprise MLPs and SVMs (general-purpose), XGBoost, LightGBM, and random forests (tabular-tailored), and CNNs (vision-tailored). All methods are trained on both modalities, except CNNs which we restrict to images. We train 200 runs per method and dataset, using randomly sampled parameters, and select the parameters for the final evaluation using 5-fold cross-validation. The full methodology for the baseline computations can be found in Appendix B.1.

4.2 Evaluation

For each dataset, we evaluate the model obtained after a single run of AML following §3. Our headline results (§5.1 and §5.2) make use of the logistic regression readout, and §5.3 compares these results with those of fewest misses empirically. For the baseline methods, the reported scores correspond to refitting to the entire train set a model with the hyperparameters selected in cross-validation. We also fit models with all the sampled hyperparameters, with the purpose of analyzing the distributions of the results. We analyze results in terms of macro- F_1 to handle class imbalance; we report macro- F_1 and accuracy results for every dataset and train-set size, for AML in both classification variants and for all baselines, in Appendix D.

For statistical significance analysis, we first apply the Friedman test [41] to test whether method ranks across datasets come from the same distribution. Following [42], we replace the conventional Nemenyi post-hoc test with pairwise two-sided Wilcoxon signed-rank tests, applying Holm’s step-down correction [43] over all $\binom{k}{2}$ pairwise comparisons among the k methods, as discussed in [41, 44]. All tests use $\alpha = 0.05$. To quantify effect sizes, we report the Hodges-Lehmann (HL) estimator of paired difference [45] (the median of pairwise averages of per-dataset differences, paired with the Wilcoxon test in the inversion-of-tests sense) and its 95% confidence interval, alongside raw and Holm-adjusted p -values. We summarize results using critical-difference diagrams [41]. All tests are computed using R’s `stats` package.

We aggregate across (dataset, training-size) pairs; per-size analyses, which avoid the assumption of independence across sizes, are reported in Appendix C.

5 Results

5.1 Image classification

Figure 1 shows, for each training-set size, the number of datasets (out of twelve) on which each method achieves the highest test F_1 macro average (top left), as well as the mean rank of each method at every size (top right). We observe strong results compared to the baselines for train set sizes 200–1000, where AML attains the highest F_1 macro average at least twice as often as every other

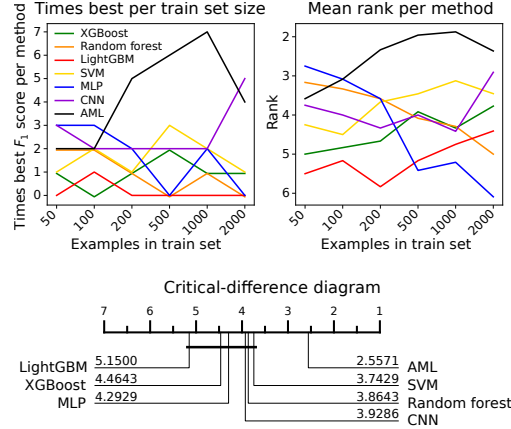


Figure 1: For image datasets, per training-set size, count of how many times each method achieved the best F_1 macro average (top left) and the mean rank of each method (top right); and critical-difference diagram for the aggregate results (bottom).

Table 1: Results of post-hoc pairwise Wilcoxon signed-rank tests for AML compared with the baseline methods on image datasets. Positive HL estimator values indicate AML achieves higher F_1 than the baselines.

Method	Raw p -value	Adjusted p -value	HL estimator	95% CI	Reject
XGBoost	< 0.001	< 0.001	+0.0269	[+0.0181, +0.0386]	Yes
Random forest	< 0.001	< 0.001	+0.0157	[+0.0099, +0.0216]	Yes
LightGBM	< 0.001	< 0.001	+0.0334	[+0.0242, +0.0466]	Yes
SVM	0.0020	0.0274	+0.0200	[+0.0072, +0.0346]	Yes
MLP	< 0.001	0.0039	+0.0269	[+0.0127, +0.0413]	Yes
CNN	< 0.001	0.0039	+0.0279	[+0.0125, +0.0503]	Yes

method. We similarly observe a large gap in the mean ranks. In this regime, standard baselines must simultaneously learn internal representations and select hyperparameters from limited data, while AML constructs algebraic structure directly from the training set with fixed hyperparameters. For the largest considered train-set size (2000 examples), we observe that CNNs become competitive with AML, which is consistent with the expectation that parametrized models exploit their task-specific biases better as data becomes more plentiful.

When aggregating the data across sizes, the Friedman test rejects the hypothesis that the ranks come from the same distribution ($p < 0.001$), and the post-hoc test (Table 1) further rejects equivalence between AML and each baseline; combined with the positive Hodges-Lehmann estimator in every comparison, this supports AML outperforming each baseline by the magnitudes reported in the table. Figure 1 bottom shows the corresponding critical-difference diagram, in which methods are sorted by mean rank and horizontal bars connect cliques that the post-hoc test cannot statistically distinguish. AML is alone in its clique; the six baselines form a single clique.

Figure 2 shows distributions of test F_1 across the 200 baseline training runs for two datasets for 100–1000 examples; the vertical lines mark the AML score and the score of the cross-validated baselines. We generally observe a wide spread of scores amongst the different train runs, particularly for smaller sizes and especially for SVMs. Nonetheless, the parameters chosen by cross-validation generally correspond to runs near the best test scores, especially for larger train-set sizes.

5.2 Tabular classification

On tabular tasks, AML’s mean rank is competitive with LightGBM and random forests and is lower than that of MLPs and SVMs at sizes greater than 200. This is noteworthy: gradient-boosted trees are widely considered the strongest standard methods for tabular prediction, and AML achieves comparable rank without data-specific biases or hyperparameter tuning.

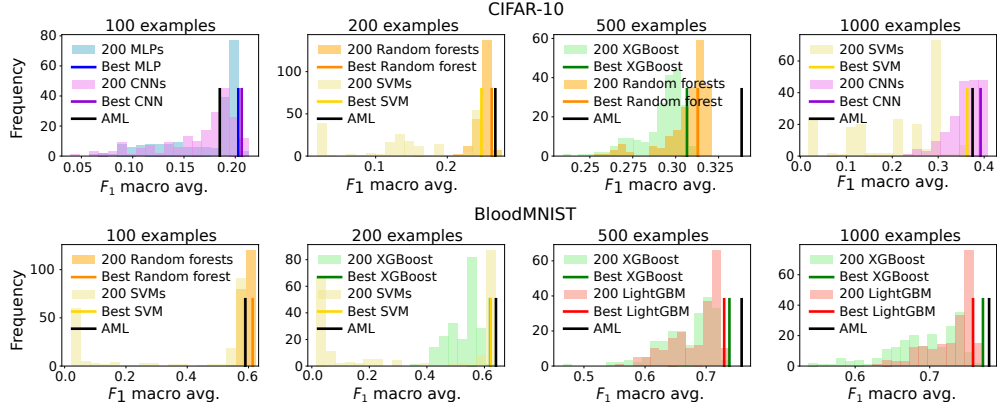


Figure 2: For image datasets, examples of distributions of F_1 scores across all runs of the two baseline models that achieved the best results in cross-validation, highlighting the results of the models trained with the hyperparameters selected in cross-validation (labeled best), and the result for AML, for sizes 100, 200, 500, and 1000.

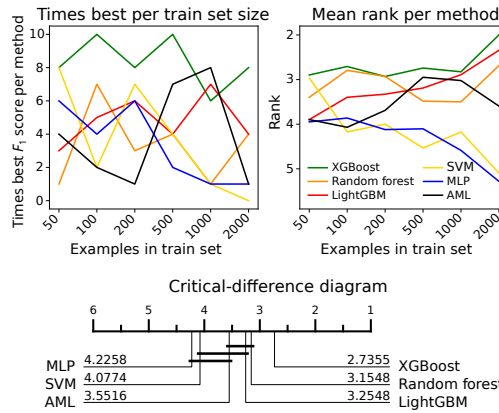


Figure 3: For tabular datasets, per training-set size, count of how many times each method achieved the best F_1 macro average (top left) and the mean rank of each method (top right); and critical-difference diagram of the aggregate results (bottom).

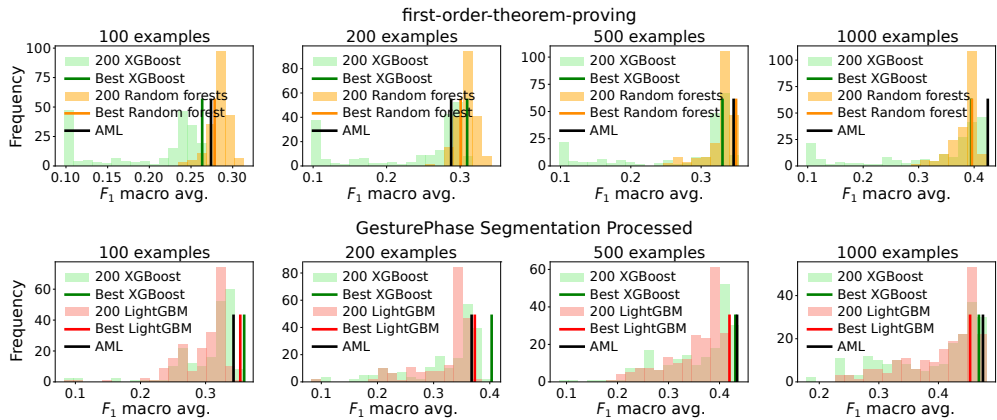


Figure 4: For tabular datasets, examples of distributions of F_1 scores across all runs of the two baseline models that achieved the best results in cross-validation, highlighting the results of the models trained with the hyperparameters selected in cross-validation (labeled best), and the result for AML, for sizes 100, 200, 500, and 1000.

Table 2: Results of post-hoc pairwise Wilcoxon signed-rank tests for AML compared with the baseline methods on tabular datasets. Positive HL estimator values indicate AML achieves higher F_1 than the baselines, and vice versa.

Method	Raw p -value	Adjusted p -value	HL estimator	95% CI	Reject
XGBoost	< 0.001	< 0.001	-0.0165	[-0.0248, -0.0091]	Yes
Random forest	0.0757	0.3029	-0.0057	[-0.0141, +0.0005]	No
LightGBM	0.2003	0.6009	-0.0049	[-0.0109, +0.0025]	No
SVM	0.0275	0.1375	+0.0115	[+0.0013, +0.0220]	No
MLP	0.0083	0.0579	+0.0139	[+0.0038, +0.0246]	No

When looking across the aggregate data, the Friedman test again rejects that the ranks come from the same distribution ($p < 0.001$), and the post-hoc test (Table 2) shows AML differs significantly from XGBoost but is comparable (in the sense that the post-hoc tests do not reject equality of distributions) to the remaining methods. Given the negative value of the HL estimator, we have evidence that XGBoost outperforms AML, but in turn we cannot deduce that AML performs differently from other domain-specific methods such as LightGBM and random forests. These relationships are summarized in the critical-difference diagram in Figure 3, bottom.

The distributions of training-run results for tabular baselines (Figure 4) show wider spread than in the image case. In the small-data regime, the cross-validation procedure often does not select the best-performing run; for example, on *first-order-theorem-proving* at 100 and 200 examples, XGBoost and random forests average F_1 macro scores of 0.2835 ($\sigma = 0.0116$) and 0.3092 ($\sigma = 0.0120$) respectively, with maxima of 0.3138 and 0.3429, but the cross-validated runs achieve 0.2784 and 0.3008.

5.3 The role of the logistic regression readout

We used a logistic regression readout as a way to classify using AML, thus a question arises regarding the role of the AML model in test classification. On image datasets, AML with the logistic regression readout achieves higher F_1 scores than the fewest misses variant on every (dataset, training-size) pair. A Wilcoxon signed-rank test rejects equivalence ($p < 0.001$), with HL estimator +0.0368 in favor of the readout (95% CI [0.0310, 0.0427]). This effect size is comparable in magnitude to AML’s HL gap over LightGBM in Table 1 (+0.0334). If we were to use fewest misses instead of the logistic regression readout as a method for classifying in AML, AML would achieve a mean rank of 4.7887, slightly better than LightGBM’s 4.8099. While the readout’s contribution is substantial, the fewest misses variant still achieves a mean rank competitive with one of the baselines.

In the case of tabular data, the logistic regression readout achieves a higher F_1 score in 89 of the 155 (dataset, training-size) pairs. The Wilcoxon signed-rank test again rejects equivalency ($p = 0.0016$), with an HL estimator of +0.0056 in favor of the logistic regression readout (95% CI [0.0020, 0.0095]). In terms of mean ranks using fewest misses instead of the logistic regression readout, AML would achieve a mean rank of 3.7516, above those of MLP and SVM (4.1806 and 4.0258 respectively), but below those of the methods that incorporate modality specific biases.

We conclude that the logistic regression readout substantially improves AML’s classification performance over the fewest misses alternative, but that the algebraic model on its own already encodes meaningful task-relevant information, achieving a mean rank competitive with several baselines (better than MLP and SVM on tabular). The choice of the logistic regression readout for our headline results in §5.1 and §5.2 reflects this performance difference.

6 Discussion

AML learns by building algebraic models of the training set rather than fitting parameters by optimization. This has two consequences in the low- to medium-data regime. First, AML requires no validation set: every labeled example is used for learning. In small-data settings where each example is precious, this is a meaningful efficiency, and it explains part of AML’s relative advantage. Second, AML’s inductive bias is fixed by the algebraic structure rather than by hyperparameters tuned on data. Cross-validated baselines must select architectures, regularization, and learning rates from limited

data. AML sidesteps the problem entirely. This explanation is consistent with the failure mode we observe in modality-tailored baselines. CNNs encode locality and translation equivariance, which should help on images regardless of training size. Yet CNNs only become competitive with AML at 2000 examples (Figure 1, top).

XGBoost has a small but statistically significant advantage over AML on tabular data, with a median paired difference of approximately 0.0165 in macro- F_1 (Table 2). This is not surprising: gradient-boosted trees encode strong, well-validated inductive biases for tabular data (additive recursive partitioning, feature-interaction handling, robustness to missing values) and have benefited from years of optimization for this exact problem class. AML, by contrast, encodes only the order relation between numerical values; everything else (categorical structure, feature interactions) must be discovered from data. That AML remains competitive with random forests and LightGBM despite this asymmetry suggests the algebraic encoding is doing real work.

The same algebraic encoding handles two structurally distinct modalities: dense pixel grids (images) and heterogeneous feature tables (tabular data). This is unusual. AML’s success across both modalities, without architectural changes, suggests the algebraic structure is modality-agnostic. A practical consequence is that a single AML model could in principle integrate features from multiple modalities without architectural redesign. We do not test this here, but the modality-agnostic encoding is a prerequisite for it, and combining heterogeneous inputs into a single algebraic structure is a direction worth exploring.

7 Limitations

We compare against standard supervised baselines trained from scratch, not few-shot, meta-learning, or transfer-learning methods that leverage auxiliary data or pretrained representations. We also do not explore the entire possible hyperparameter space for these models, or other potential ways to improve results for parametrized learners such as ensembles of methods.

AML’s reported performance uses a logistic regression readout on top of the algebraic atomization; §5.3 reports a comparison with the fewest misses classification method that more directly uses the information from the underlying algebra and shows that the algebraic model encodes meaningful task-relevant information independently of the readout. Nonetheless, our experiments do not fully isolate the readout’s contribution from that of the atomization, nor do they disentangle those of the algebraic encoding, rule-finding bias, and the absence of cross-validation; controlled ablations are needed. AML’s task encoding is part of its inductive bias, and identifying the most effective encodings for these and new problem classes remains open.

In a similar line, the symbolic algebraic encoding necessary for AML is well-suited to supervised classification tasks, but implementing other kinds of tasks often requires significant work to build tailor-made algebraic embeddings.

Our aggregated statistical analysis treats (dataset, training-size) pairs as approximately independent observations. Performance on the same dataset at adjacent sizes is correlated, which may make our p -values mildly anti-conservative.

Finally, the current implementation of Sparse Crossing prioritizes a direct realization of the algebraic construction over runtime efficiency. Runtime and memory use for images with dimensionality higher than what we analyze here grow beyond the capabilities of the desktop-class systems available to us. Larger image datasets may require algorithmic acceleration, parallelization, or dedicated hardware implementations. We view this primarily as a systems challenge for a new algebraic learning framework: AML has not yet benefited from the extensive optimization effort that has made deep learning, gradient-boosted trees, and other parametrized methods efficient. Closing this gap is an important direction for future work.

8 Conclusion

We have shown that Algebraic Machine Learning [9, 10, 11] — a symbolic framework that learns through algebraic decomposition rather than numerical parameter fitting — is the best-performing method on image classification across the 50–2000 example range we evaluate, and is competitive with domain-specific tabular methods such as random forests and LightGBM in the same range,

though XGBoost outperforms it on tabular data overall. Because the same encoding framework is used across both modalities, these results point to a generic algebraic inductive bias that is effective when labeled data are scarce, helped by AML’s lack of hyperparameter tuning and validation requirements.

The methods AML competes with have benefited from decades of architectural refinement, optimized implementations, and hardware co-design. AML, by contrast, has a single unoptimized implementation, generic encodings, and no task-specific engineering. We view its current competitiveness as evidence that algebraic decomposition is a viable learning mechanism in the regimes we test; whether and how the framework scales to larger data, additional modalities, or more diverse task types is an empirical question that future work will need to answer.

Acknowledgments

We thank Antonio Ricciardo, Nabil Abderrahaman Elena and Emilio Suarez Canedo for discussions. We are grateful for the support from Champalimad Foundation (Lisbon, Portugal), from FCT – Fundação para a Ciência e a Tecnologia – in the context of the project UIDB/04443/2025, and from the European Commission provided through projects H2020 ICT48 *Humane AI; Toward AI Systems That Augment and Empower Humans by Understanding Us, our Society and the World Around Us* (grant #820437) and the H2020 ICT48 project *ALMA: Human Centric Algebraic Machine Learning* (grant #952091).

References

- [1] Christopher M. Bishop. *Pattern Recognition and Machine Learning (Information Science and Statistics)*. Springer-Verlag, Berlin, Heidelberg, 2006.
- [2] Ian Goodfellow, Yoshua Bengio, and Aaron Courville. *Deep Learning*. MIT Press, 2016. <http://www.deeplearningbook.org>.
- [3] Tianqi Chen and Carlos Guestrin. Xgboost: A scalable tree boosting system. *Proceedings of the 22nd ACM SIGKDD International Conference on Knowledge Discovery and Data Mining*, 2016.
- [4] Leo Breiman. Random forests. *Mach. Learn.*, 45(1):5–32, October 2001.
- [5] Corinna Cortes and Vladimir Vapnik. Support-vector networks. *Machine learning*, 20(3):273–297, 1995.
- [6] Allen Newell and Herbert A. Simon. Computer science as empirical inquiry: symbols and search. *Commun. ACM*, 19(3):113–126, March 1976.
- [7] Edward A. Feigenbaum. The art of artificial intelligence: Themes and case studies of knowledge engineering. In *International Joint Conference on Artificial Intelligence*, 1977.
- [8] Frederick Hayes-Roth, Donald A. Waterman, and Douglas B. Lenat. *Building expert systems*. Addison-Wesley Longman Publishing Co., Inc., USA, 1983.
- [9] Fernando Martin-Maroto and Gonzalo G. de Polavieja. Algebraic machine learning. *arXiv:1803.05252*, 2018.
- [10] Fernando Martin-Maroto and Gonzalo G de Polavieja. Finite atomized semilattices. *arXiv:2102.08050*, 2021.
- [11] Fernando Martin-Maroto and Gonzalo G de Polavieja. Semantic embeddings in semilattices. *arXiv:2205.12618*, 2022.
- [12] Y. Lecun, L. Bottou, Y. Bengio, and P. Haffner. Gradient-based learning applied to document recognition. *Proceedings of the IEEE*, 86(11):2278–2324, 1998.
- [13] Guolin Ke, Qi Meng, Thomas Finley, Taifeng Wang, Wei Chen, Weidong Ma, Qiwei Ye, and Tie-Yan Liu. Lightgbm: a highly efficient gradient boosting decision tree. In *Proceedings of the 31st International Conference on Neural Information Processing Systems, NIPS’ 17*, page 3149–3157, Red Hook, NY, USA, 2017. Curran Associates Inc.
- [14] Chelsea Finn, Pieter Abbeel, and Sergey Levine. Model-agnostic meta-learning for fast adaptation of deep networks. In *Proceedings of the 34th International Conference on Machine Learning - Volume 70, ICML’ 17*, page 1126–1135. JMLR.org, 2017.

- [15] Ting Chen, Simon Kornblith, Mohammad Norouzi, and Geoffrey Hinton. A simple framework for contrastive learning of visual representations. In *Proceedings of the 37th International Conference on Machine Learning*, ICML'20. JMLR.org, 2020.
- [16] Ryan Riegel, Alexander G. Gray, Francois P. S. Luus, Naweed Khan, Ndivhuwo Makondo, Ismail Yunus Akhalwaya, Haifeng Qian, Ronald Fagin, Francisco Barahona, Udit Sharma, Shajith Iqbal, Hima Karanam, Sumit Neelam, Ankita Likhyan, and Santosh K. Srivastava. Logical neural networks. *arXiv:2006.13155*, 2020.
- [17] Samy Badreddine, Artur d'Avila Garcez, Luciano Serafini, and Michael Spranger. Logic tensor networks. *Artificial Intelligence*, 303:103649, 2022.
- [18] Taco S. Cohen and Max Welling. Group equivariant convolutional networks. In *Proceedings of the 33rd International Conference on International Conference on Machine Learning - Volume 48*, ICML'16, page 2990–2999. JMLR.org, 2016.
- [19] Mathias Drton, Bernd Sturmfels, and Seth Sullivant. *Lectures on Algebraic Statistics*. Birkhäuser Basel, 2009.
- [20] Brendan Fong and David I. Spivak. *An Invitation to Applied Category Theory: Seven Sketches in Compositionality*. Cambridge University Press, 2019.
- [21] Fernando Martin-Maroto, Nabil Abderrahaman, David Mendez, and Gonzalo G. de Polavieja. Algebraic machine learning: Learning as computing an algebraic decomposition of a task. *arXiv:2502.19944*, 2025.
- [22] Stanley Burris and H. P. Sankappanavar. *A course in universal algebra*. Springer-Verlag, 1981.
- [23] B. A. Davey and H. A. Priestley. *Introduction to Lattices and Order*. Cambridge University Press, 2 edition, 2002.
- [24] Garrett Birkhoff. Subdirect products in universal algebra. *Bull. Amer. Math. Soc.*, 50:764–768, 1944.
- [25] Yann LeCun, Corinna Cortes, and CJ Burges. Mnist handwritten digit database. *ATT Labs [Online]*. Available: <http://yann.lecun.com/exdb/mnist>, 2, 2010.
- [26] Tarin Clanuwat, Mikel Bober-Irizar, Asanobu Kitamoto, Alex Lamb, Kazuaki Yamamoto, and David Ha. Deep learning for classical japanese literature. *arXiv:1812.01718*, 2018.
- [27] Andrea Acevedo, Anna Merino, Santiago Alférez, Ángel Molina, Laura Boldú, and José Rodellar. A dataset of microscopic peripheral blood cell images for development of automatic recognition systems. *Data in Brief*, 30:105474, 2020.
- [28] Xuanang Xu, Fugen Zhou, Bo Liu, Dongshan Fu, and Xiangzhi Bai. Efficient multiple organ localization in ct image using 3d region proposal network. *IEEE Transactions on Medical Imaging*, 38(8):1885–1898, 2019.
- [29] Daniel S. Kermany, Michael Goldbaum, Wenjia Cai, Carolina C.S. Valentim, Huiying Liang, Sally L. Baxter, Alex McKeown, Ge Yang, Xiaokang Wu, Fangbing Yan, Justin Dong, Made K. Prasadha, Jacqueline Pei, Magdalene Y.L. Ting, Jie Zhu, Christina Li, Sierra Hewett, Jason Dong, Ian Ziyar, Alexander Shi, Runze Zhang, Lianghong Zheng, Rui Hou, William Shi, Xin Fu, Yaou Duan, Viet A.N. Huu, Cindy Wen, Edward D. Zhang, Charlotte L. Zhang, Oulan Li, Xiaobo Wang, Michael A. Singer, Xiaodong Sun, Jie Xu, Ali Tafreshi, M. Anthony Lewis, Huimin Xia, and Kang Zhang. Identifying medical diagnoses and treatable diseases by image-based deep learning. *Cell*, 172(5):1122–1131.e9, 2018.
- [30] Philipp Tschandl, Cliff Rosendahl, and Harald Kittler. The ham10000 dataset, a large collection of multi-source dermatoscopic images of common pigmented skin lesions. *Scientific Data*, 5(1), August 2018.
- [31] Noel Codella, Veronica Rotemberg, Philipp Tschandl, M. Emre Celebi, Stephen Dusza, David Gutman, Brian Helba, Aadi Kalloo, Konstantinos Liopyris, Michael Marchetti, Harald Kittler, and Allan Halpern. Skin lesion analysis toward melanoma detection 2018: A challenge hosted by the international skin imaging collaboration (isic). *arXiv:1902.03368*, 2019.
- [32] Jiancheng Yang, Rui Shi, Donglai Wei, Zequan Liu, Lin Zhao, Bilian Ke, Hanspeter Pfister, and Bingbing Ni. Medmnist v2—a large-scale lightweight benchmark for 2d and 3d biomedical image classification. *Scientific Data*, 10(1):41, 2023.
- [33] Alex Krizhevsky. Learning multiple layers of features from tiny images. Technical report, 2009.

- [34] Han Xiao, Kashif Rasul, and Roland Vollgraf. Fashion-mnist: a novel image dataset for benchmarking machine learning algorithms. *arXiv:1708.07747*, 2017.
- [35] Adam Coates, Andrew Ng, and Honglak Lee. An analysis of single-layer networks in unsupervised feature learning. In *International Conference on Artificial Intelligence and Statistics*, 2011.
- [36] Will Cukierski. Aerial cactus identification. <https://kaggle.com/competitions/aerial-cactus-identification>, 2019. Kaggle.
- [37] Efrén López-Jiménez, Juan Irving Vasquez-Gomez, Miguel Angel Sanchez-Acevedo, Juan Carlos Herrera-Lozada, and Abril Valeria Uriarte-Arcia. Columnar cactus recognition in aerial images using a deep learning approach. *Ecological Informatics*, 52:131–138, 2019.
- [38] Yuval Netzer, Tao Wang, Adam Coates, A. Bissacco, Bo Wu, and A. Ng. Reading digits in natural images with unsupervised feature learning. 2011.
- [39] S.A. Nene, S.K. Nayar, and H. Murase. Columbia Object Image Library (COIL-20). In *Technical Report, Department of Computer Science, Columbia University UCUS-005-96*, Feb 1996.
- [40] Noah Hollmann, Samuel Müller, Lennart Purucker, Arjun Krishnakumar, Max Körfer, Shi Bin Hoo, Robin Tibor Schirmer, and Frank Hutter. Accurate predictions on small data with a tabular foundation model. *Nature*, 637(8045):319–326, January 2025.
- [41] Janez Demšar. Statistical comparisons of classifiers over multiple data sets. *J. Mach. Learn. Res.*, 7:1–30, December 2006.
- [42] Alessio Benavoli, Giorgio Corani, and Francesca Mangili. Should we really use post-hoc tests based on mean-ranks? *Journal of Machine Learning Research*, 17(5):1–10, 2016.
- [43] Sture Holm. A simple sequentially rejective multiple test procedure. *Scandinavian Journal of Statistics*, 6(2):65–70, 1979.
- [44] Salvador García and Francisco Herrera. An extension on “statistical comparisons of classifiers over multiple data sets” for all pairwise comparisons. *Journal of Machine Learning Research*, 9(89):2677–2694, 2008.
- [45] Myles Hollander, Douglas A. Wolfe, and Eric Chicken. *Nonparametric Statistical Methods*. Wiley, 2015.
- [46] Isabelle Guyon, Lisheng Sun-Hosoya, Marc Boullé, Hugo Jair Escalante, Sergio Escalera, Zhengying Liu, Damir Jajetic, Bisakha Ray, Mehreen Saeed, Michèle Sebag, Alexander Statnikov, Wei-Wei Tu, and Evelyne Viegas. *Analysis of the AutoML Challenge Series 2015–2018*, pages 177–219. Springer International Publishing, Cham, 2019.
- [47] Ross Quinlan. Statlog (Australian Credit Approval). UCI Machine Learning Repository, 1987. DOI: <https://doi.org/10.24432/C59012>.
- [48] I-Cheng Yeh, King-Jang Yang, and Tao-Ming Ting. Knowledge discovery on rfm model using bernoulli sequence. *Expert Systems with Applications*, 36(3, Part 2):5866–5871, 2009.
- [49] Marko Bohanec and Vladislav Rajkovic. Knowledge acquisition and explanation for multi-attribute decision making. In *8th intl workshop on expert systems and their applications*, pages 59–78. Avignon France, 1988.
- [50] Unknown. Churn. OpenML Dataset Repository. OpenML ID: 40701.
- [51] Tjen-Sien Lim. Contraceptive Method Choice. UCI Machine Learning Repository, 1999. DOI: <https://doi.org/10.24432/C59W2D>.
- [52] Hans Hofmann. Statlog (German Credit Data). UCI Machine Learning Repository, 1994. DOI: <https://doi.org/10.24432/C5NC77>.
- [53] Molecular Biology (Splice-junction Gene Sequences). UCI Machine Learning Repository, 1991. DOI: <https://doi.org/10.24432/C5M888>.
- [54] Blake Bulloch. Eucalyptus species selection for soil conservation in seasonally dry hill country - twelfth year assessment. *New Zealand journal of forestry science*, 21:10–31, 1991.
- [55] James Bridge, Sean Holden, and Lawrence Paulson. First-order theorem proving. UCI Machine Learning Repository, 2012. DOI: <https://doi.org/10.24432/C5RC9X>.

- [56] Renata C. B. Madeo, Clodoaldo A. M. Lima, and Sarajane M. Peres. Gesture unit segmentation using support vector machines: segmenting gestures from rest positions. In *Proceedings of the 28th Annual ACM Symposium on Applied Computing, SAC '13*, page 46–52, New York, NY, USA, 2013. Association for Computing Machinery.
- [57] Isabelle Guyon, Kristin Bennett, Gavin Cawley, {Hugo Jair} Escalante, Sergio Escalera, {Tin Kam} Ho, Núria Macià, Bisakha Ray, Mehreen Saeed, Alexander Statnikov, and Evelyne Viegas. Design of the 2015 chlearn automl challenge. In *2015 International Joint Conference on Neural Networks, IJCNN 2015*, Proceedings of the International Joint Conference on Neural Networks, United States, September 2015. IEEE Signal Processing Society. Publisher Copyright: © 2015 IEEE.; International Joint Conference on Neural Networks, IJCNN 2015 ; Conference date: 12-07-2015 Through 17-07-2015.
- [58] Nan Niu and A. Mahmoud. Enhancing candidate link generation for requirements tracing: The cluster hypothesis revisited. In *Requirements Engineering Conference (RE), 2012 20th IEEE International*, pages 81–90, Sept 2012.
- [59] Alen Shapiro. Chess (King-Rook vs. King-Pawn). UCI Machine Learning Repository, 1983. DOI: <https://doi.org/10.24432/C5DK5C>.
- [60] Robert Duin. Multiple Features. UCI Machine Learning Repository, 1998. DOI: <https://doi.org/10.24432/C5HC70>.
- [61] Kun Zhang, Wei Fan, and XiaoJing Yuan. Ozone Level Detection. UCI Machine Learning Repository, 2008. DOI: <https://doi.org/10.24432/C5NG6W>.
- [62] T. Menzies and J.S. Di Stefano. How good is your blind spot sampling policy. In *High Assurance Systems Engineering, 2004. Proceedings. Eighth IEEE International Symposium on*, pages 129–138, March 2004.
- [63] Pierre Alinat and Jean-Marie Pierrel. Esprit ii project 5516 roars robust analytic speech recognition system. 1994.
- [64] Kamel Mansouri, Tine Ringsted, Davide Ballabio, Roberto Todeschini, and Viviana Consonni. QSAR biodegradation. UCI Machine Learning Repository, 2013. DOI: <https://doi.org/10.24432/C5H60M>.
- [65] Markus Goldstein. Unsupervised Anomaly Detection Benchmark, 2015.
- [66] Image Segmentation. UCI Machine Learning Repository, 1990. DOI: <https://doi.org/10.24432/C5GP4N>.
- [67] M Buscema, S Terzi, and W Tastle. Steel Plates Faults. UCI Machine Learning Repository, 2010. DOI: <https://doi.org/10.24432/C5J88N>.
- [68] Jan Paul Siebert. Vehicle recognition using rule based methods, project report. In *Turing Institute, Glasgow*, 1987.
- [69] Brian Johnson. Wilt. UCI Machine Learning Repository, 2013. DOI: <https://doi.org/10.24432/C5KS4M>.
- [70] P. Cortez, Antonio Luíz Cerdeira, Fernando Almeida, Telmo Matos, and José Reis. Modeling wine preferences by data mining from physicochemical properties. *Decis. Support Syst.*, 47:547–553, 2009.
- [71] Kenta Nakai. Yeast. UCI Machine Learning Repository, 1991. DOI: <https://doi.org/10.24432/C5KG68>.

A Datasets characteristics

Table 3 contains the characteristics of the analyzed image datasets. The train/validation/test splits are irrelevant for our purposes as we only take examples from the train dataset. All datasets are provided under a license allowing for research use, including CC BY-SA 3.0 (MNIST), CC BY-SA 4.0 (Kuzushiji-49), CC-BY 4.0 (BloodMNIST, OrganCMNIST, PneumoniaMNIST), CC BY-NC 4.0 (DermaMNIST), MIT (Fashion-MNIST, CIFAR-10), CC0 (Street view house number), GPL-2 (Aerial Cactus Identification) and other/unknown licenses allowing for academic use (STL-10, COIL-20).

Table 3: Characteristics of analyzed image datasets, including their domain, resolution, color channels, the number of test examples, the number of targets and the ratio between the most and least common examples in the test split.

Dataset	Domain	Res. & channels	Test set	Targets	Ratio
MNIST [25]	Handwriting recognition	28 × 28, 1	10000	10	1.27
Kuzushiji-49 [26]	Handwriting recognition	28 × 28, 1	38547	49	15.63
BloodMNIST [27, 32]	Medical images	28 × 28, 3	3421	8	2.74
OrganCMNIST [28, 32]	Medical images	28 × 28, 1	8216	11	4.36
PneumoniaMNIST [29, 32]	Medical images	28 × 28, 1	624	2	1.67
DermaMNIST [30, 31, 32]	Medical images	28 × 28, 3	2005	8	2.74
CIFAR-10 [33]	Object recognition	32 × 32, 3	10000	10	1.00
Fashion-MNIST [34]	Object recognition	28 × 28, 1	10000	10	1.00
STL-10 [35]	Object recognition	32 × 32, 3	8000	10	1.00
Aerial cactus identification [36, 37]	Object recognition	32 × 32, 3	10000	2	3.09
Street view house number [38]	Number recognition	32 × 32, 3	26032	10	3.20
COIL-20 [39]	Object recognition	128 × 128, 1	440	20	1.00

Table 4 contains the characteristics of the analyzed tabular datasets. All datasets were acquired from OpenML and are displayed using their names in OpenML; OpenML identifiers are available in [40, Extended Data Table 3]. Many of these datasets are part of the UCI Machine Learning Repository and are available under the CC-BY 4.0 license (Australian, blood-transfusion, car, cmc, credit-g, dna, first-order-theorem-proving, Gesture Phase Segmentation Processed, kr-vs-kp, mfeat-factors, ozone-level-8hr, qsar-biodeg, segment, steel-plates-fault, vehicle, wilt, yeast). Several datasets have origin in the AutoML challenges and do not have an explicit license, but are nonetheless of frequent use in research (ada, jasmine, madeline, philippine, sylvine). Satellite is released under the CC0 license, and wine-quality-white under the Database Contents License (DbCL) 1.0. The datasets kc1, pc4 and phoneme originate from old research projects (NASA PROMISE for kc1 and pc4; EU ELENA for phoneme) and have no disclosed licenses. Finally, churn and eucalyptus have no known license. All datasets are of frequent use in research, but those with undisclosed licenses may not be suitable for commercial use.

B Methodology for experiments

B.1 Baseline methods

In both image and tabular datasets, hyperparameters for the final parametrized models were chosen via stratified 5-fold cross-validation, using Scikit-learn, with 200 runs per method. Hyperparameters were sampled randomly within reasonable ranges. Image datasets were normalized so that the train dataset in each case has a mean of 0 and a standard deviation of 1. For tabular datasets, and for methods that do not admit categorical features (MLPs, SVMs), each possible value of the categorical features was mapped to a fixed integer value. For these methods, the data was then normalized so that each variable in the training dataset has a mean of 0 and a standard deviation of 1. We now outline, for each of the methods, the computational tools and parameter ranges sampled; any omitted hyperparameter was left as default in the corresponding software libraries.

Table 4: Characteristics of analyzed tabular datasets, including their domain, number of features, how many of them are categorical, the number of test examples, the number of targets and the ratio between the most and least common examples in the test split.

Dataset	Domain	Feats.	Cat. feats.	Test set	Targets	Ratio
ada [46]	Census	48	0	415	2	2.71
Australian [47]	Finance	14	8	69	2	1.03
blood-transfusion -service-center [48]	Healthcare	4	0	75	2	3.41
car [49]	Automotive	6	6	173	4	20.67
churn [50]	Telecommunication	20	4	500	2	5.41
cmc [51]	Public health	9	7	148	3	2.00
credit-g [52]	Finance	20	13	100	2	1.63
dna [53]	Biology	180	180	319	3	2.41
eucalyptus [54]	Agriculture	19	5	74	5	1.5
first-order -theorem-proving [55]	Computational logic	51	0	612	6	5.1
Gesture Phase segmen- -tation processed [56]	Human-computer interaction	32	0	988	5	3.82
jasmine [57]	Natural language processing	144	136	299	2	1.03
kc1 [58]	Software engineering	21	0	211	2	4.86
kr-vs-kp [59]	Game strategy	36	36	320	2	1.03
madeline [57]	Synthetic	259	0	314	2	1.11
mfeat-factors [60]	Handwriting recognition	216	0	200	10	1.86
ozone-level-8hr [61]	Environmental	72	0	254	2	20.17
pc4 [62]	Software engineering	37	0	146	2	9.43
philippine [57]	Bioinformatics	308	0	584	2	1.01
phoneme [63]	Audio	5	0	541	2	2.66
qsar-biodeg [64]	Environmental	41	0	106	2	2.12
Satellite [65]	Environmental Science	36	0	510	2	126.5
segment [66]	Computer Vision	16	0	231	7	1.37
steel-plates-fault [67]	Industrial	27	0	195	7	17.5
sylvine [57]	Environmental Science	20	0	513	2	1.06
vehicle [68]	Image classification	18	0	85	4	1.63
wilt [69]	Environmental	5	0	484	2	19.17
wine-quality-white [70]	Food and beverage	11	0	490	7	105.00
yeast [71]	Biology	8	0	149	10	25.00

XGBoost. Computations were performed using the Python `xgboost` library’s Scikit-learn API. All parameters were uniformly sampled, other than the learning rate, which was sampled from a loguniform distribution. The parameter ranges are `colsample_bytree` from 0.6 to 1, `max_depth` from 3 to 20, `gamma` from 0 to 0.01, `learning_rate/eta` from 0.001 to 0.2, `n_estimators` from 50 to 500, `reg_alpha` from 0 to 2, `reg_lambda` from 0 to 2 and `subsample` from 0.6 to 1.

LightGBM. Computations were similarly performed using the Python `lightgbm` library’s Scikit-learn API. Considered ranges are the same as those used in XGBoost, and `num_leaves` was sampled in the range from 20 to 50.

Random forests. We used Scikit-learn’s `RandomForestClassifier`. All parameters are uniformly sampled, with ranges `max_depth` from 3 to 20, `n_estimators` from 50 to 500, `min_samples_split` from 2 to 10, and `min_samples_leaf` from 1 to 4.

SVMs. Computations were performed using the `SVC` method from Scikit-learn. The kernel is randomly sampled for each run between linear, radial basis function (rbf), sigmoid and polynomial.

The regularization parameter C is sampled to be loguniform in the range of 0.1 to 100. For sigmoid, rbf and polynomial kernels, γ is sampled from a loguniform in the range 0.001 to 10. For the polynomial kernel, the degree is uniformly sampled in the range from 2 to 5. We used 12 as the penalty.

MLPs. MLP computations were made using the `skorch` library, providing an API between Pytorch and Scikit-learn, thus allowing for the usage of Scikit-learn’s cross-validation methods. Learning rate was uniformly sampled in the interval $(10^{-5}, 10^{-4})$, and layer sizes were uniformly selected from 128, 256, 512, 2048 or 4096 for the first hidden layer, 128, 256, 1024 or 2048 for the second hidden layer, 0, 128, 256 or 512 for the third hidden layer and 0, 128 or 256 for the fourth hidden layer. Thus, on average we can expect 50 models to be two layers deep, 100 models to be three layers deep and 50 models to be four layers deep. Intermediate layers use ReLU as the activation function. Training was done for a maximum of 50 epochs, and the epoch with the best validation accuracy was recorded for each run. The final model for which metrics are reported is trained with the hyperparameters that achieved the best cross-validation results, for a number of epochs equal to the mean of the epochs used in cross-validation. The models were trained using the ADAM optimizer with a batch size of 128, with the parameters `betas` and `eps` left as default in Pytorch.

CNNs. CNN computations were performed only on image datasets, with the same tooling used for MLPs, and we used the same learning rate interval, optimizer, and batch size. We used a linear classifier of fixed size with 2 hidden layers, of sizes 128 and 64. We used two to three convolutional layers, with square kernel sizes sampled from 3, 5 and 7 for the first two layers, and from 0, 3 and 5 for the third layer. We can thus expect an average of 100 runs with 2 convolutional layers, and another 100 runs with 3 layers. ReLU was used for the activation functions, and intermediate convolutional layers use dropout with a value of 0.2 for normalization.

Other than the SVMs, all methods were trained minimizing cross-entropy loss. The reported best test results correspond to a model trained on the entire train dataset, using the hyperparameters of the model that achieved the best average results between the five cross-validation runs. To ensure train samples were balanced between the different classes, for all methods except for MLPs and CNNs, train samples used at each epoch were sampled from the corresponding train dataset with a weight corresponding to their inverse prevalence in the dataset, whereas for MLPs and CNNs the loss was scaled according to the inverse prevalence of each of the classes.

All baseline computations were performed on a system with an AMD Epyc 7301 CPU with 128 GB of RAM and an NVIDIA GTX 1080 Ti GPU. GPU acceleration was used for XGBoost, MLPs and CNNs, the remaining methods were run on CPU with a number of workers equal to the number of CPU physical threads. RAM usage was not observed to surpass 32 GB during the course of the experiments. Run times varied substantially between datasets and training set sizes, ranging from a few seconds to around 24 hours per dataset and training set size, mostly when running XGBoost on datasets with 2000 train examples.

B.2 AML

The general procedure and parameter selection (batch number, batch size growth, post-training model reduction, logistic regression readout) is introduced in §3.3, and except for batch sizes mostly matches [21, Methods]. For our experiments we used an internal development version of Algebraic AI’s Open AML Engine (<https://github.com/Algebraic-AI/Open-AML-Engine>) with additional optimizations that reduce runtime particularly when dealing with numerical values and their order relations. Any hyperparameters mentioned in [21, Methods] not disclosed in §3.3 (simplification threshold, union model fractioning parameter) were left as their default for image classification tasks (1.5 and 0.1 respectively).

All experiments were run on a system with an AMD Ryzen 5 5950X CPU with 128 GB of RAM and an NVIDIA RTX 3090 GPU. The Open AML engine does not make use of GPU acceleration and is single threaded in a lot of its tasks, so we typically ran two datasets concurrently. The GPU was used to train the logistic regression readout, which was trained using Pytorch with the ADAM optimizer.

Overall runtime per dataset varied widely between different datasets and training set sizes, ranging from a few minutes to around one week per dataset and training set size, mainly when running image datasets with 2000 train examples. Tabular datasets often run faster, typically finishing an entire

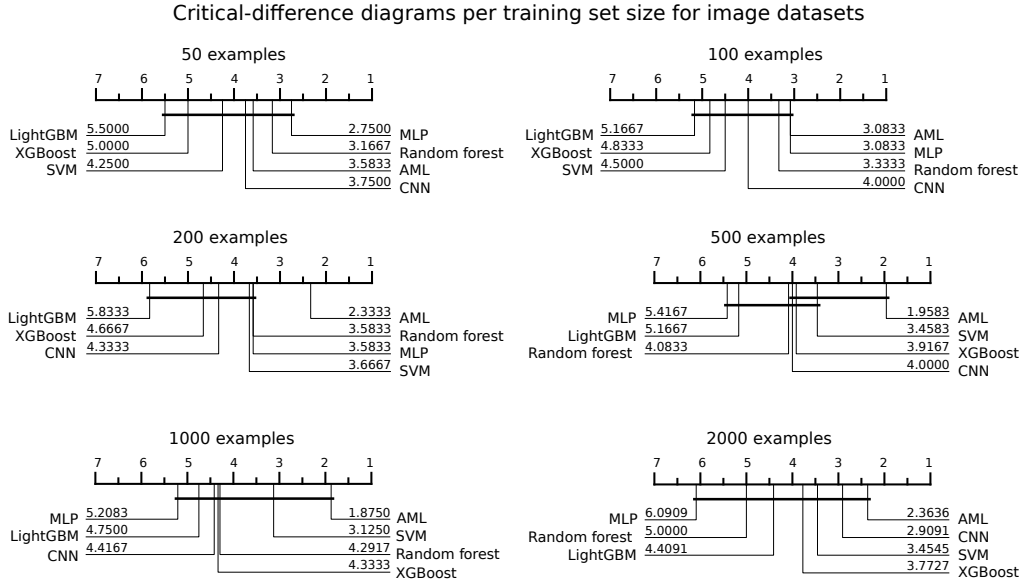


Figure 5: For image datasets, and per each of the considered training set sizes, critical-difference diagram including all analyzed methods, using the logistic regression readout as the AML classification variant.

train and evaluation run with 2000 train examples in 48 to 72 hours. We did not observe RAM usage surpassing 64 GB for a single dataset. Most of the runtime was used for training, with model reduction typically taking 1 to 2 hours and inference taking 2 to 4 hours for the larger datasets, including training the logistic regression readout.

C Per size statistical analysis

In this section we provide statistical analysis and critical-difference diagrams per size of train dataset, for both image and tabular datasets. All per-size analyses use the same methodology as the aggregated analysis described in §4.2: Friedman omnibus test with pairwise two-sided Wilcoxon signed-rank tests with Holm correction over all $\binom{k}{2}$ pairs as post-hoc, at $\alpha = 0.05$. Critical-difference diagrams use the same procedure for clique formation.

C.1 Image datasets

We observe that the Friedman test does not reject the hypothesis that the ranks come from the same distribution for size $n = 100$ at $\alpha = 0.05$ ($p = 0.0770$). The test rejects for all other sizes. We still report the post-hoc tables and critical-difference diagrams for illustrative purposes.

The main conclusion we can draw from the analysis is that AML is consistently in the clique with the best-ranked methods in the critical-difference diagram. Nonetheless, given the reduced number of datasets, in most cases there is only one clique, so no two methods can be distinguished by the Wilcoxon test. Note that, due to the inherent limitations of critical-difference diagrams as one-dimensional representations, if two methods are not distinguishable but can nonetheless be distinguished from a third method whose rank lies between them, a clique may not be drawn between the first two non-distinguishable methods. We observe this for the 200-example image setting: AML and MLP are not statistically distinguishable from each other (Table 5), but the diagram cannot show this because Random forest, which is distinguishable from AML, shares its rank position.

The per-size critical-difference diagrams can be found in Figure 5; and the tables for the post-hoc statistics can be found in Table 5 (sizes 50–200) and Table 6 (sizes 500–2000).

Table 5: Per train set size, results of Friedman and post-hoc pairwise Wilcoxon signed-rank tests for AML compared with the baseline methods on image datasets, for sizes between 50 and 200 examples. Positive HL estimator values indicate AML achieves higher F_1 than the baselines, and vice versa.

Friedman test p -value: 0.0208						
	Method	Raw p -value	Adj. p -value	HL estimator	95% CI	Reject
50 examples	XGBoost	0.0342	0.5469	+0.0607	[+0.0009, +0.1361]	No
	Random forest	0.9697	1.0000	-0.0016	[-0.0228, +0.0136]	No
	LightGBM	0.0122	0.2197	+0.0602	[+0.0106, +0.1405]	No
	SVM	0.5693	1.0000	+0.0121	[-0.0378, +0.1521]	No
	MLP	0.7334	1.0000	-0.0040	[-0.0381, +0.0236]	No
	CNN	0.2334	1.0000	+0.0241	[-0.0165, +0.1259]	No
Friedman test p -value: 0.0770 (does not reject)						
	Method	Raw p -value	Adj. p -value	HL estimator	95% CI	Reject
100 examples	XGBoost	0.0269	0.5371	+0.0331	[+0.0044, +0.1008]	No
	Random forest	0.8501	1.000	+0.0020	[-0.0144, +0.0306]	No
	LightGBM	0.0161	0.3384	+0.0414	[+0.0093, +0.1134]	No
	SVM	0.1514	1.0000	+0.0378	[-0.0220, +0.0833]	No
	MLP	0.8501	1.0000	+0.0051	[-0.0271, +0.0530]	No
	CNN	0.1294	1.0000	+0.0202	[-0.0037, +0.1661]	No
Friedman test p -value: 0.0053						
	Method	Raw p -value	Adj. p -value	HL estimator	95% CI	Reject
200 examples	XGBoost	0.0024	0.0464	+0.0347	[+0.0149, +0.0638]	Yes
	Random forest	< 0.001	0.0205	+0.0145	[+0.0051, +0.0297]	Yes
	LightGBM	0.0015	0.0293	+0.0464	[+0.0223, +0.0907]	Yes
	SVM	0.0923	1.0000	+0.0206	[-0.0044, +0.0545]	No
	MLP	0.4697	1.0000	+0.0096	[-0.0190, +0.0574]	No
	CNN	0.2661	1.0000	+0.0293	[-0.0210, +0.0796]	No

C.2 Tabular datasets

We similarly observe that the Friedman test does not reject the hypothesis that the ranks come from the same distribution for one of the sizes at $\alpha = 0.05$, in this case for $n = 50$ ($p = 0.0819$).

We observe in this case that XGBoost is consistently the algorithm with the best mean rank, with AML not being distinguishable from XGBoost in any size. In fact, AML is not distinguishable from any method at any individual training-set size, even though the aggregated analysis (Table 2) distinguishes AML from XGBoost. This reflects the lower statistical power of per-size analyses compared to aggregated analysis. The per-size critical-difference diagrams can be found in Figure 6, and the tables for the post-hoc statistics can be found in Table 7.

D Extended experimental results

In Table 8 we provide accuracies and F_1 scores for all image datasets, for the single AML run as well as for the models selected after hyperparameter selection for all the parametrized baselines. We provide the same information for tabular datasets in Table 9. Note that not all tabular datasets are large enough to reserve 1000 or 2000 training examples, and similarly only 1000 examples were reserved for training in COIL-20.

Table 6: Per train set size, results of Friedman and post-hoc pairwise Wilcoxon signed-rank tests for AML compared with the baseline methods on image datasets, for sizes between 500 and 2000 examples. Positive HL estimator values indicate AML achieves higher F_1 than the baselines, and vice versa.

		Friedman test p -value: 0.0026				
	Method	Raw p -value	Adj. p -value	HL estimator	95% CI	Reject
500 examples	XGBoost	0.0269	0.4297	+0.0259	[+0.0016, +0.0516]	No
	Random forest	< 0.001	0.0103	+0.0217	[+0.0112, +0.0375]	Yes
	LightGBM	0.0034	0.0615	+0.0344	[+0.0138, +0.0612]	No
	SVM	0.2300	1.0000	+0.0235	[-0.0069, +0.1572]	No
	MLP	< 0.001	0.0103	+0.0489	[+0.0148, +0.0849]	Yes
	CNN	0.0122	0.2075	+0.0579	[+0.0038, +0.1109]	No

		Friedman test p -value: 0.0027				
	Method	Raw p -value	Adj. p -value	HL estimator	95% CI	Reject
1000 examples	XGBoost	0.0210	0.3989	+0.0225	[+0.0082, +0.0406]	No
	Random forest	0.0051	0.1020	+0.0241	[+0.0126, +0.0353]	No
	LightGBM	0.0034	0.0718	+0.0246	[+0.0093, +0.0410]	No
	SVM	0.1681	1.0000	+0.0115	[-0.0090, +0.0570]	No
	MLP	0.0454	0.7726	+0.0430	[+0.0039, +0.0765]	No
	CNN	0.0342	0.6152	+0.0293	[+0.0018, +0.0900]	No

		Friedman test p -value: < 0.001				
	Method	Raw p -value	Adj. p -value	HL estimator	95% CI	Reject
2000 examples	XGBoost	0.0674	1.0000	+0.0124	[-0.0063, +0.0313]	No
	Random forest	0.0137	0.2598	+0.0314	[+0.0113, +0.0479]	No
	LightGBM	0.0674	1.0000	+0.0159	[-0.0035, +0.0313]	No
	SVM	0.2061	1.0000	+0.0126	[-0.0162, +0.0290]	No
	MLP	0.0322	0.5479	+0.0595	[+0.0073, +0.1002]	No
	CNN	0.7002	1.0000	+0.0031	[-0.0759, +0.0612]	No

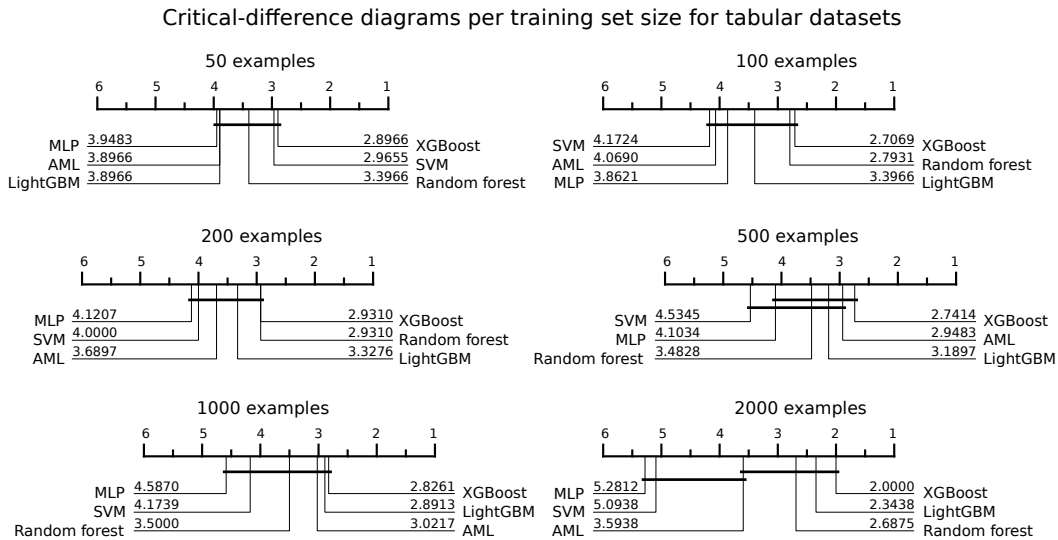


Figure 6: For tabular datasets, and per each of the considered training set sizes, critical-difference diagram including all analyzed methods, using the logistic regression readout as the AML classification variant.

Table 7: Per train set size, results of Friedman and post-hoc pairwise Wilcoxon signed-rank tests for AML compared with the baseline methods on tabular datasets. Positive HL estimator values indicate AML achieves higher F_1 than the baselines, and vice versa.

Friedman test p -value: 0.0819 (does not reject)						
50 examples	Method	Raw p -value	Adj. p -value	HL estimator	95% CI	Reject
	XGBoost	0.1056	1.0000	-0.0200	[-0.0415, +0.0048]	No
	Random forest	0.5221	1.0000	-0.0090	[-0.0463, +0.0210]	No
	LightGBM	0.5504	1.0000	+0.0129	[-0.0199, +0.0454]	No
	SVM	0.3467	1.0000	-0.0175	[-0.0555, +0.0250]	No
	MLP	0.8382	1.0000	+0.0038	[-0.0368, +0.0531]	No
Friedman test p -value: 0.0044						
100 examples	Method	Raw p -value	Adj. p -value	HL estimator	95% CI	Reject
	XGBoost	0.0065	0.0968	-0.0337	[-0.0563, -0.0104]	No
	Random forest	0.0111	0.1556	-0.0299	[-0.0536, -0.0062]	No
	LightGBM	0.1035	0.8279	-0.0114	[-0.0280, +0.0021]	No
	SVM	0.8480	1.0000	-0.0017	[-0.0329, +0.0273]	No
	MLP	0.7172	1.0000	-0.0058	[-0.0334, +0.0253]	No
Friedman test p -value: 0.0472						
200 examples	Method	Raw p -value	Adj. p -value	HL estimator	95% CI	Reject
	XGBoost	0.0543	0.6939	-0.0167	[-0.0332, +0.0009]	No
	Random forest	0.1683	1.0000	-0.0079	[-0.0224, +0.0050]	No
	LightGBM	0.4047	1.0000	-0.0060	[-0.0206, +0.0092]	No
	SVM	0.4420	1.0000	+0.0102	[-0.0135, +0.0323]	No
	MLP	0.1557	1.0000	+0.0139	[-0.0059, +0.0373]	No
Friedman test p -value: 0.0012						
500 examples	Method	Raw p -value	Adj. p -value	HL estimator	95% CI	Reject
	XGBoost	0.3467	1.0000	-0.0093	[-0.0301, +0.0068]	No
	Random forest	0.4593	1.0000	+0.0028	[-0.0055, +0.0138]	No
	LightGBM	0.6391	1.0000	-0.0044	[-0.0228, +0.0129]	No
	SVM	0.0052	0.0739	+0.0259	[+0.0073, +0.0453]	No
	MLP	0.1982	1.0000	+0.0120	[-0.0073, +0.0404]	No
Friedman test p -value: 0.0033						
1000 examples	Method	Raw p -value	Adj. p -value	HL estimator	95% CI	Reject
	XGBoost	0.8967	1.0000	+0.0011	[-0.0277, +0.0158]	No
	Random forest	0.5399	1.0000	+0.0061	[-0.0126, +0.0327]	No
	LightGBM	0.5600	1.0000	+0.0059	[-0.0107, +0.0265]	No
	SVM	0.0149	0.1784	+0.0194	[+0.0040, +0.0458]	No
	MLP	0.0049	0.0679	+0.0252	[+0.0067, +0.0611]	No
Friedman test p -value: < 0.001						
2000 examples	Method	Raw p -value	Adj. p -value	HL estimator	95% CI	Reject
	XGBoost	0.0110	0.0879	-0.0164	[-0.0751, -0.0046]	No
	Random forest	0.2744	0.9772	-0.0091	[-0.0314, +0.0076]	No
	LightGBM	0.0063	0.0566	-0.0123	[-0.0567, -0.0033]	No
	SVM	0.0156	0.1085	+0.0256	[+0.0070, +0.0592]	No
	MLP	0.0214	0.1286	+0.0387	[+0.0090, +0.0677]	No

Table 8: Experimental results in accuracy and macro- F_1 for image datasets, for AML in both classification variants and baselines. The headline results for AML use the logistic regression readout; results obtained via fewest misses are also reported.

	# train	AML		Fewest misses		XGBoost		LightGBM		Random Forest		SVM		MLP		CNN	
		acc.	F_1	acc.	F_1	acc.	F_1	acc.	F_1	acc.	F_1	acc.	F_1	acc.	F_1	acc.	F_1
MNIST	50	60.74%	0.5903	57.37%	0.5537	43.99%	0.4263	51.22%	0.5001	61.45%	0.5955	64.22%	0.6298	63.32%	0.6220	66.37%	0.6537
	100	66.72%	0.6436	64.07%	0.6081	62.08%	0.6058	60.46%	0.5872	68.44%	0.6614	68.42%	0.6675	69.87%	0.6849	67.66%	0.6578
	200	75.75%	0.7433	74.16%	0.7240	71.49%	0.7063	70.15%	0.6934	74.09%	0.7250	77.59%	0.7651	77.27%	0.7623	78.86%	0.7835
	500	86.76%	0.8655	83.67%	0.8339	82.28%	0.8197	80.77%	0.8044	83.77%	0.8334	87.57%	0.8744	86.01%	0.8580	86.41%	0.8624
	1000	90.74%	0.9061	88.79%	0.8863	87.82%	0.8767	87.58%	0.8740	88.60%	0.8841	91.30%	0.9118	89.34%	0.8916	90.57%	0.9044
	2000	92.99%	0.9290	91.43%	0.9130	90.91%	0.9081	91.34%	0.9124	91.76%	0.9164	93.72%	0.9363	89.40%	0.8921	93.75%	0.9364
Fashion-MNIST	50	62.65%	0.6187	59.17%	0.5806	51.29%	0.5020	48.88%	0.4736	62.92%	0.6275	66.00%	0.6605	67.83%	0.6748	64.67%	0.6479
	100	69.12%	0.6929	66.15%	0.6597	62.66%	0.6289	63.87%	0.6419	70.34%	0.7040	57.65%	0.6069	71.63%	0.7195	65.33%	0.6561
	200	74.74%	0.7471	73.05%	0.7328	70.77%	0.7108	70.64%	0.7096	74.61%	0.7428	75.58%	0.7573	75.07%	0.7517	67.58%	0.6514
	500	79.14%	0.7892	77.60%	0.7739	76.99%	0.7705	76.71%	0.7664	78.13%	0.7767	78.96%	0.7890	78.81%	0.7888	79.22%	0.7916
	1000	81.74%	0.8162	79.69%	0.7964	80.43%	0.8048	79.65%	0.7964	79.78%	0.7946	81.25%	0.8132	76.63%	0.7687	79.67%	0.7946
	2000	83.78%	0.8362	81.63%	0.8147	82.85%	0.8281	82.85%	0.8281	82.39%	0.8211	82.85%	0.8289	81.58%	0.8170	83.08%	0.8319
CIFAR-10	50	18.00%	0.1571	16.79%	0.1450	15.46%	0.1532	15.33%	0.1464	20.76%	0.1858	19.09%	0.1657	20.18%	0.1805	19.53%	0.1736
	100	21.31%	0.1849	20.26%	0.1614	19.10%	0.1787	19.22%	0.1840	22.04%	0.2017	17.44%	0.1145	21.99%	0.2029	22.05%	0.2062
	200	27.61%	0.2671	26.34%	0.2432	24.12%	0.2355	23.10%	0.2250	27.14%	0.2620	26.32%	0.2477	25.33%	0.2416	25.35%	0.2417
	500	34.68%	0.3384	33.12%	0.3164	31.65%	0.3066	30.40%	0.2960	32.73%	0.3129	30.14%	0.2981	28.40%	0.2699	31.71%	0.3016
	1000	38.01%	0.3748	36.39%	0.3554	35.57%	0.3508	34.35%	0.3386	35.64%	0.3467	36.46%	0.3634	31.87%	0.3113	39.12%	0.3922
	2000	42.58%	0.4223	39.49%	0.3869	40.30%	0.3996	39.31%	0.3911	38.48%	0.3746	40.53%	0.4052	36.08%	0.3577	44.29%	0.4420
OrganCMNIST	50	54.53%	0.4544	47.59%	0.3830	34.63%	0.2640	32.92%	0.2621	53.71%	0.4403	22.33%	0.0332	44.97%	0.3867	46.68%	0.4002
	100	60.35%	0.5273	56.58%	0.4904	47.77%	0.4191	46.68%	0.4018	56.89%	0.4973	49.04%	0.4363	51.89%	0.4542	57.08%	0.5133
	200	71.41%	0.6953	66.15%	0.6248	63.90%	0.6185	61.09%	0.5868	69.06%	0.6668	63.05%	0.6160	60.11%	0.5803	60.56%	0.5804
	500	76.22%	0.7477	71.86%	0.6999	71.84%	0.7016	71.25%	0.6980	73.04%	0.7141	70.24%	0.6927	63.44%	0.6173	68.61%	0.6298
	1000	79.99%	0.7850	75.47%	0.7356	74.74%	0.7333	75.49%	0.7392	76.76%	0.7496	74.31%	0.7281	67.76%	0.6559	76.36%	0.7408
	2000	82.45%	0.8102	78.42%	0.7709	79.35%	0.7788	80.26%	0.7875	78.60%	0.7685	76.79%	0.7539	69.07%	0.6700	80.79%	0.7830

	# train	AML		Fewest misses		XGBoost		LightGBM		Random Forest		SVM		MLP		CNN	
		acc.	F_1	acc.	F_1	acc.	F_1	acc.	F_1	acc.	F_1	acc.	F_1	acc.	F_1	acc.	F_1
BloodMNIST	50	51.33%	0.4613	48.52%	0.4057	46.80%	0.4251	44.90%	0.4065	53.99%	0.4733	46.62%	0.4179	49.17%	0.4468	51.68%	0.4868
	100	65.21%	0.5897	63.81%	0.5440	59.78%	0.5652	59.89%	0.5438	66.71%	0.6134	63.46%	0.5860	54.49%	0.4780	51.86%	0.4210
	200	72.03%	0.6399	67.85%	0.5513	69.10%	0.6199	66.30%	0.5837	67.49%	0.5916	67.20%	0.6213	61.03%	0.5167	63.72%	0.5158
	500	79.63%	0.7581	75.36%	0.7024	77.52%	0.7381	77.02%	0.7295	74.45%	0.6836	74.31%	0.7066	64.25%	0.6169	68.14%	0.6450
	1000	81.29%	0.7796	76.79%	0.7171	80.01%	0.7714	79.04%	0.7581	76.82%	0.7377	77.40%	0.7430	74.74%	0.7172	74.04%	0.6709
	2000	85.12%	0.8311	80.06%	0.7639	83.89%	0.8188	83.72%	0.8143	80.24%	0.7772	82.52%	0.8021	71.56%	0.6953	81.53%	0.7684
DermaMNIST	50	59.90%	0.1939	63.84%	0.1780	54.16%	0.1965	54.36%	0.1943	60.00%	0.1809	46.63%	0.1675	54.66%	0.1940	58.60%	0.1879
	100	66.18%	0.2344	66.33%	0.1803	59.05%	0.2224	60.50%	0.2508	65.99%	0.2033	66.88%	0.1145	58.15%	0.2089	52.77%	0.2229
	200	66.48%	0.2453	67.43%	0.2054	62.19%	0.2535	64.49%	0.2528	67.28%	0.1911	66.88%	0.1145	60.30%	0.2456	62.49%	0.2103
	500	68.58%	0.2716	68.18%	0.2227	56.16%	0.3047	52.17%	0.2883	68.18%	0.2291	66.88%	0.1145	65.99%	0.1749	66.93%	0.1354
	1000	69.18%	0.2862	69.63%	0.2549	62.34%	0.3293	54.56%	0.2997	69.33%	0.2373	67.53%	0.1549	65.49%	0.2656	69.53%	0.2149
	2000	70.47%	0.3124	70.47%	0.2609	61.75%	0.3830	57.41%	0.3507	69.68%	0.2442	69.63%	0.2770	67.88%	0.1919	67.28%	0.1317
PneumoniaMNIST	50	74.04%	0.6726	71.31%	0.6081	75.32%	0.7069	71.31%	0.6500	72.92%	0.6485	76.12%	0.7087	80.93%	0.7796	62.50%	0.3846
	100	80.77%	0.7709	78.37%	0.7324	83.17%	0.8100	80.45%	0.7744	75.00%	0.6858	84.29%	0.8297	74.20%	0.6582	62.82%	0.3939
	200	78.53%	0.7376	77.40%	0.7166	76.44%	0.7207	75.16%	0.7137	77.88%	0.7260	77.72%	0.7245	83.17%	0.8081	82.85%	0.8049
	500	83.49%	0.8077	82.53%	0.7922	84.78%	0.8245	83.49%	0.8082	83.49%	0.8071	83.81%	0.8124	79.49%	0.7485	77.08%	0.7037
	1000	84.29%	0.8162	82.53%	0.7916	83.33%	0.8066	83.17%	0.8071	82.85%	0.8002	83.81%	0.8086	81.89%	0.7805	81.89%	0.7783
	2000	85.26%	0.8280	83.97%	0.8108	83.97%	0.8135	83.97%	0.8135	84.13%	0.8167	85.58%	0.8322	80.93%	0.7642	83.97%	0.8073
Aerial Cactus Identification	50	79.93%	0.6279	79.32%	0.5863	77.74%	0.6696	75.88%	0.6663	82.80%	0.7010	87.44%	0.8034	79.28%	0.5970	75.53%	0.4303
	100	83.50%	0.7175	82.91%	0.6948	80.16%	0.7206	78.72%	0.6976	83.75%	0.7107	89.46%	0.8475	83.26%	0.7720	78.73%	0.5539
	200	86.84%	0.7851	85.32%	0.7458	86.21%	0.7916	85.22%	0.7779	86.65%	0.7827	89.89%	0.8523	86.95%	0.8195	93.68%	0.9113
	500	90.77%	0.8602	88.78%	0.8194	90.56%	0.8665	89.88%	0.8531	90.31%	0.8574	91.26%	0.8711	88.49%	0.8415	93.95%	0.9185
	1000	91.67%	0.8787	90.57%	0.8557	89.65%	0.8563	91.14%	0.8752	90.85%	0.8661	92.08%	0.8879	85.91%	0.8225	94.67%	0.9258
	2000	92.43%	0.8913	91.41%	0.8706	92.49%	0.8976	92.28%	0.8954	90.65%	0.8664	92.60%	0.8947	88.85%	0.8456	96.29%	0.9497

	# train	AML		Fewest misses		XGBoost		LightGBM		Random Forest		SVM		MLP		CNN	
		acc.	F_1	acc.	F_1	acc.	F_1	acc.	F_1	acc.	F_1	acc.	F_1	acc.	F_1	acc.	F_1
Street View House Number	50	13.66%	0.1024	12.93%	0.0900	12.14%	0.1015	12.81%	0.1048	14.62%	0.1194	15.17%	0.1047	15.67%	0.1240	15.94%	0.0275
	100	17.27%	0.1226	17.03%	0.1002	14.74%	0.1235	14.52%	0.1240	18.05%	0.1372	15.94%	0.0275	20.18%	0.1618	20.58%	0.1334
	200	20.27%	0.1552	19.67%	0.1256	16.29%	0.1354	17.04%	0.1368	20.04%	0.1416	19.83%	0.1149	21.37%	0.1638	18.90%	0.0637
	500	28.96%	0.2189	25.80%	0.1722	22.94%	0.1868	24.08%	0.1908	27.61%	0.2007	32.00%	0.2714	29.14%	0.2080	19.59%	0.0328
	1000	35.96%	0.3038	30.66%	0.2410	30.88%	0.2654	32.51%	0.2745	35.93%	0.3097	41.42%	0.3785	45.78%	0.4250	19.46%	0.0330
	2000	43.70%	0.3907	38.66%	0.3219	43.67%	0.3904	43.82%	0.3877	47.06%	0.4224	51.49%	0.4793	53.36%	0.5119	75.03%	0.7232
STL-10	50	22.45%	0.2179	20.31%	0.1873	17.81%	0.1700	17.62%	0.1680	22.49%	0.1977	10.00%	0.0182	22.60%	0.2003	19.65%	0.1770
	100	23.95%	0.2181	23.42%	0.2047	20.50%	0.1947	20.51%	0.1938	25.11%	0.2290	18.54%	0.1466	23.81%	0.2177	22.24%	0.1937
	200	30.16%	0.2945	29.28%	0.2826	26.34%	0.2560	26.12%	0.2551	29.91%	0.2893	28.58%	0.2708	27.94%	0.2777	26.16%	0.2304
	500	35.09%	0.3379	33.44%	0.3169	32.57%	0.3178	31.51%	0.3100	33.36%	0.3201	33.64%	0.3304	30.40%	0.2984	33.71%	0.3313
	1000	39.14%	0.3866	36.64%	0.3591	36.49%	0.3641	35.33%	0.3545	35.83%	0.3542	36.31%	0.3639	28.88%	0.2897	36.81%	0.3666
	2000	42.94%	0.4254	39.99%	0.3909	41.40%	0.4131	39.56%	0.3959	38.74%	0.3753	40.79%	0.4022	36.94%	0.3604	41.92%	0.4047
Kuzushiji-49	50	18.72%	0.1252	15.08%	0.0911	6.92%	0.0465	7.09%	0.0469	16.15%	0.1000	17.66%	0.1163	19.90%	0.1358	19.91%	0.1362
	100	22.78%	0.1710	16.15%	0.1290	9.71%	0.0703	9.64%	0.0697	21.84%	0.1692	16.82%	0.1205	22.76%	0.1767	24.18%	0.1839
	200	32.58%	0.2650	25.06%	0.2037	16.61%	0.1309	16.06%	0.1256	32.80%	0.2667	28.10%	0.2178	28.75%	0.2438	31.73%	0.2607
	500	42.87%	0.3742	36.22%	0.2909	29.67%	0.2461	28.56%	0.2351	40.71%	0.3523	9.75%	0.0372	37.94%	0.3282	42.33%	0.3691
	1000	48.71%	0.4357	42.49%	0.3565	38.17%	0.3244	35.69%	0.3058	48.19%	0.4292	48.40%	0.4295	45.91%	0.4124	44.47%	0.4088
	2000	55.41%	0.5117	48.67%	0.4250	48.05%	0.4287	47.22%	0.4202	53.45%	0.4841	54.05%	0.4934	54.30%	0.5050	57.05%	0.5277
COIL-20	50	69.32%	0.6606	58.41%	0.5541	44.77%	0.3893	43.18%	0.3792	69.55%	0.6623	52.95%	0.5085	64.77%	0.6133	65.00%	0.6143
	100	84.09%	0.8413	78.18%	0.7570	63.64%	0.6210	62.05%	0.5926	83.64%	0.8262	83.41%	0.8357	82.95%	0.8285	83.86%	0.8357
	200	94.77%	0.9468	90.91%	0.9042	87.73%	0.8679	81.36%	0.8009	92.50%	0.9237	92.95%	0.9267	91.36%	0.9104	92.73%	0.9275
	500	99.55%	0.9955	98.64%	0.9864	93.86%	0.9381	92.73%	0.9256	98.86%	0.9885	99.55%	0.9955	98.86%	0.9885	99.09%	0.9908
	1000	100.00%	1.0000	99.32%	0.9932	99.32%	0.9932	99.32%	0.9932	100.00%	1.0000	100.00%	1.0000	100.00%	1.0000	99.55%	0.9954

Table 9: Experimental results in accuracy and macro- F_1 for tabular datasets, for AML in both classification variants and for the baselines. The headline results for AML use the logistic regression readout; results obtained via fewest misses are also reported.

	# train	AML		Fewest misses		XGBoost		LightGBM		Random Forest		SVM		MLP	
		acc.	F_1	acc.	F_1	acc.	F_1	acc.	F_1	acc.	F_1	acc.	F_1	acc.	F_1
ada	50	71.08%	0.6310	71.81%	0.6433	74.94%	0.7123	66.75%	0.6183	77.83%	0.7304	73.25%	0.7090	79.76%	0.7513
	100	75.90%	0.7151	77.59%	0.7254	78.80%	0.7556	75.90%	0.7276	79.04%	0.7333	71.57%	0.6542	75.90%	0.7084
	200	77.11%	0.7054	78.55%	0.7154	74.94%	0.7253	71.08%	0.6919	79.28%	0.7454	71.81%	0.6160	73.98%	0.6865
	500	82.17%	0.7725	82.17%	0.7656	80.00%	0.7630	80.96%	0.7713	82.65%	0.7733	76.14%	0.7298	78.80%	0.7177
	1000	82.65%	0.7747	82.89%	0.7730	78.31%	0.7548	81.93%	0.7877	82.65%	0.7786	80.00%	0.7640	81.20%	0.7691
	2000	83.13%	0.7769	83.13%	0.7710	82.65%	0.7984	81.69%	0.7881	83.86%	0.7969	80.00%	0.7640	81.20%	0.7514
Australian	50	72.46%	0.7244	73.91%	0.7391	88.41%	0.8834	86.96%	0.8678	86.96%	0.8686	88.41%	0.8829	86.96%	0.8686
	100	78.26%	0.7826	79.71%	0.7971	84.06%	0.8404	85.51%	0.8550	85.51%	0.8550	84.06%	0.8384	85.51%	0.8543
	200	89.86%	0.8986	88.41%	0.8840	89.86%	0.8986	89.86%	0.8985	91.30%	0.9129	86.96%	0.8695	91.30%	0.9130
	500	91.30%	0.9130	91.30%	0.9130	86.96%	0.8696	86.96%	0.8695	92.75%	0.9275	86.96%	0.8686	91.30%	0.9130
blood-transfusion-service-center	50	77.33%	0.6832	76.00%	0.6577	64.00%	0.5817	49.33%	0.4722	66.67%	0.6032	76.00%	0.6828	80.00%	0.6612
	100	74.67%	0.6460	74.67%	0.6460	73.33%	0.6345	73.33%	0.6591	73.33%	0.6028	76.00%	0.5813	76.00%	0.6577
	200	72.00%	0.5921	72.00%	0.5921	66.67%	0.6032	66.67%	0.5925	73.33%	0.6345	77.33%	0.5920	77.33%	0.6698
	500	68.00%	0.5436	68.00%	0.5436	70.67%	0.6462	73.33%	0.6865	74.67%	0.6903	78.67%	0.5385	80.00%	0.6794
car	50	78.03%	0.4419	79.77%	0.4694	74.57%	0.4573	54.34%	0.3222	77.46%	0.4843	80.35%	0.5689	80.35%	0.5266
	100	83.82%	0.6193	83.24%	0.6186	89.60%	0.7884	82.08%	0.6267	86.71%	0.6711	88.44%	0.6980	90.17%	0.7635
	200	89.02%	0.6992	88.44%	0.6732	89.02%	0.7568	90.17%	0.7577	92.49%	0.7757	91.91%	0.7725	93.06%	0.8080
	500	94.22%	0.8309	91.91%	0.6847	93.64%	0.8283	95.95%	0.8834	94.80%	0.8425	96.53%	0.9156	95.38%	0.9038
	1000	98.84%	0.9332	98.84%	0.9332	96.53%	0.8969	97.11%	0.9014	97.69%	0.9059	97.69%	0.9240	98.27%	0.9203
churn	50	83.40%	0.5508	84.20%	0.4921	79.40%	0.5355	69.40%	0.5049	84.80%	0.4837	79.20%	0.6315	84.40%	0.4577
	100	84.00%	0.6266	85.00%	0.6010	83.00%	0.6167	80.60%	0.5947	84.20%	0.5650	85.20%	0.5482	84.40%	0.4577
	200	86.40%	0.6471	87.00%	0.6356	87.40%	0.7668	84.00%	0.6368	87.00%	0.6599	86.80%	0.6459	86.80%	0.6733
	500	88.00%	0.7159	87.80%	0.7048	88.20%	0.7794	83.60%	0.7529	88.80%	0.7185	87.00%	0.7145	87.20%	0.7054
	1000	88.00%	0.6984	88.20%	0.6693	92.40%	0.8476	93.80%	0.8778	92.00%	0.8159	88.80%	0.7587	88.40%	0.7038
	2000	88.80%	0.7140	87.00%	0.6220	93.80%	0.8841	95.20%	0.9038	94.80%	0.8920	91.00%	0.8097	89.60%	0.8174

	# train	AML		Fewest misses		XGBoost		LightGBM		Random Forest		SVM		MLP	
		acc.	F_1	acc.	F_1	acc.	F_1	acc.	F_1	acc.	F_1	acc.	F_1	acc.	F_1
cmc	50	43.92%	0.4342	44.59%	0.4403	47.30%	0.4738	35.81%	0.3516	43.92%	0.4351	42.57%	0.4136	46.62%	0.4403
	100	52.03%	0.5181	52.70%	0.5260	47.97%	0.4774	49.32%	0.4924	48.65%	0.4861	47.30%	0.4723	48.65%	0.4842
	200	50.68%	0.5074	53.38%	0.5379	47.97%	0.4800	47.30%	0.4748	47.30%	0.4754	54.05%	0.5448	52.03%	0.5213
	500	50.68%	0.4963	52.70%	0.5134	50.68%	0.5062	49.32%	0.4918	47.30%	0.4761	44.59%	0.4468	52.03%	0.5043
	1000	56.76%	0.5350	56.08%	0.5321	49.32%	0.4901	46.62%	0.4701	49.32%	0.4960	52.03%	0.5149	52.70%	0.5281
credit-g	50	60.00%	0.4667	56.00%	0.3789	57.00%	0.4725	58.00%	0.5000	61.00%	0.4729	63.00%	0.5131	60.00%	0.4667
	100	65.00%	0.5793	66.00%	0.5784	67.00%	0.6397	62.00%	0.6194	67.00%	0.6349	59.00%	0.3711	72.00%	0.6727
	200	70.00%	0.6608	71.00%	0.6640	67.00%	0.6692	70.00%	0.6956	71.00%	0.6792	68.00%	0.6435	71.00%	0.6580
	500	71.00%	0.6695	74.00%	0.6905	71.00%	0.7050	65.00%	0.6457	74.00%	0.6843	66.00%	0.6212	71.00%	0.6938
dna	50	59.25%	0.5648	57.68%	0.5226	86.21%	0.8527	62.38%	0.6168	84.64%	0.8273	75.55%	0.7285	69.59%	0.6266
	100	81.19%	0.7938	80.56%	0.7910	85.89%	0.8534	82.45%	0.8175	84.95%	0.8357	78.68%	0.7634	79.94%	0.7715
	200	89.03%	0.8808	85.89%	0.8427	89.34%	0.8898	87.15%	0.8630	88.71%	0.8780	86.52%	0.8552	85.27%	0.8372
	500	91.85%	0.9136	91.22%	0.9069	91.22%	0.9086	89.34%	0.8869	91.85%	0.9126	91.85%	0.9131	90.91%	0.9022
	1000	90.60%	0.9001	91.54%	0.9089	91.22%	0.9063	90.91%	0.9042	92.48%	0.9192	91.54%	0.9097	90.91%	0.9008
	2000	92.79%	0.9236	92.16%	0.9164	93.42%	0.9267	93.10%	0.9240	93.42%	0.9255	93.10%	0.9232	92.16%	0.9119
eucalyptus	50	47.30%	0.4563	44.59%	0.4474	40.54%	0.4217	32.43%	0.3010	35.14%	0.3614	41.89%	0.4119	45.95%	0.3859
	100	50.00%	0.4677	54.05%	0.5159	51.35%	0.5165	52.70%	0.5092	56.76%	0.5706	58.11%	0.5876	64.86%	0.6331
	200	55.41%	0.5362	67.57%	0.6670	58.11%	0.5751	56.76%	0.5617	60.81%	0.6042	62.16%	0.6202	55.41%	0.5482
	500	70.27%	0.6953	71.62%	0.7041	71.62%	0.7173	70.27%	0.7022	68.92%	0.6902	62.16%	0.6084	72.97%	0.7139
first-order-theorem-proving	50	37.75%	0.2181	39.22%	0.1946	38.89%	0.2569	35.95%	0.2644	37.91%	0.2186	41.99%	0.1352	41.67%	0.0980
	100	39.38%	0.2740	43.30%	0.2814	37.25%	0.2634	27.61%	0.2390	42.32%	0.2784	41.18%	0.1759	37.42%	0.2571
	200	39.54%	0.2878	41.01%	0.2816	38.73%	0.3096	39.38%	0.2960	43.79%	0.3008	41.83%	0.2148	40.03%	0.2738
	500	44.77%	0.3462	44.93%	0.3327	40.69%	0.3304	37.42%	0.3151	42.32%	0.3497	39.38%	0.2854	41.50%	0.3019
	1000	53.10%	0.4246	51.80%	0.4018	47.39%	0.3946	39.54%	0.3346	50.33%	0.3959	46.24%	0.3414	47.06%	0.3196
	2000	55.39%	0.4434	56.05%	0.4423	52.12%	0.4353	52.94%	0.4395	54.58%	0.4462	44.44%	0.3582	49.51%	0.3723

	# train	AML		Fewest misses		XGBoost		LightGBM		Random Forest		SVM		MLP	
		acc.	F_1	acc.	F_1	acc.	F_1	acc.	F_1	acc.	F_1	acc.	F_1	acc.	F_1
GesturePhase Segmentation Processed	50	37.85%	0.3079	39.17%	0.3018	36.34%	0.3211	36.54%	0.3217	39.98%	0.3143	37.96%	0.3020	37.55%	0.2654
	100	42.81%	0.3429	41.50%	0.3160	38.97%	0.3592	37.55%	0.3533	42.61%	0.3473	41.90%	0.2617	42.41%	0.3219
	200	48.48%	0.3676	49.29%	0.3507	47.67%	0.4033	42.31%	0.3733	48.89%	0.3666	40.79%	0.3473	47.77%	0.3607
	500	52.33%	0.4344	51.82%	0.3921	48.58%	0.4310	45.85%	0.4195	52.33%	0.3911	47.17%	0.3999	48.28%	0.3132
	1000	54.25%	0.4747	54.25%	0.4413	52.43%	0.4679	48.48%	0.4531	54.45%	0.4292	48.79%	0.3846	50.20%	0.4431
	2000	58.30%	0.5256	56.28%	0.4905	58.70%	0.5382	57.69%	0.5356	57.09%	0.4833	51.11%	0.4323	47.17%	0.4313
jasmine	50	69.90%	0.6987	69.23%	0.6919	74.92%	0.7490	76.92%	0.7690	74.92%	0.7492	79.93%	0.7962	73.58%	0.7355
	100	69.90%	0.6972	70.57%	0.7039	77.93%	0.7787	70.23%	0.7021	79.26%	0.7894	78.60%	0.7790	76.59%	0.7647
	200	76.25%	0.7623	77.93%	0.7788	79.93%	0.7981	80.27%	0.8021	79.93%	0.7962	80.94%	0.8034	73.24%	0.7323
	500	78.26%	0.7825	79.26%	0.7918	81.94%	0.8185	81.61%	0.8151	81.61%	0.8144	79.93%	0.7965	77.93%	0.7793
	1000	80.94%	0.8089	80.27%	0.8014	82.27%	0.8218	82.27%	0.8209	81.61%	0.8149	80.60%	0.8007	80.60%	0.8060
	2000	82.61%	0.8259	84.28%	0.8424	84.62%	0.8452	83.28%	0.8318	82.61%	0.8242	80.27%	0.8016	77.59%	0.7759
kc1	50	84.36%	0.6049	83.41%	0.5468	83.89%	0.5305	82.94%	0.5608	82.94%	0.5433	83.89%	0.6004	82.94%	0.4534
	100	79.15%	0.4418	82.46%	0.4519	78.20%	0.5968	80.09%	0.5802	83.41%	0.5272	83.89%	0.5084	82.94%	0.4534
	200	80.09%	0.5676	81.99%	0.5833	78.67%	0.6742	73.46%	0.6279	80.57%	0.5428	83.41%	0.5056	83.41%	0.5468
	500	81.52%	0.6362	81.52%	0.6045	64.93%	0.5851	69.19%	0.6115	82.94%	0.6052	82.94%	0.5241	83.41%	0.6224
	1000	82.46%	0.6718	81.99%	0.6088	73.93%	0.6371	68.25%	0.6038	81.99%	0.5833	83.41%	0.5468	82.94%	0.4534
kr-vs-kp	50	87.81%	0.8776	83.12%	0.8288	88.12%	0.8811	59.69%	0.5962	85.00%	0.8500	75.00%	0.7496	51.88%	0.3832
	100	84.69%	0.8468	84.38%	0.8437	90.31%	0.9031	85.94%	0.8591	91.56%	0.9156	83.12%	0.8307	87.81%	0.8781
	200	95.00%	0.9500	94.69%	0.9469	97.19%	0.9719	95.00%	0.9500	95.31%	0.9531	91.88%	0.9187	90.94%	0.9094
	500	97.81%	0.9781	97.81%	0.9781	98.44%	0.9844	98.12%	0.9812	97.50%	0.9750	95.31%	0.9531	96.56%	0.9656
	1000	98.75%	0.9875	98.44%	0.9844	99.06%	0.9906	99.69%	0.9969	98.75%	0.9875	96.88%	0.9687	96.88%	0.9687
	2000	98.75%	0.9875	98.75%	0.9875	99.38%	0.9937	99.38%	0.9937	98.44%	0.9844	98.12%	0.9812	98.12%	0.9812

	# train	AML		Fewest misses		XGBoost		LightGBM		Random Forest		SVM		MLP	
		acc.	F_1	acc.	F_1	acc.	F_1	acc.	F_1	acc.	F_1	acc.	F_1	acc.	F_1
madeline	50	50.64%	0.5064	50.00%	0.5000	46.82%	0.4672	43.63%	0.4342	50.32%	0.5030	52.87%	0.5280	54.14%	0.5414
	100	46.82%	0.4636	47.13%	0.4576	50.96%	0.5062	47.13%	0.4658	51.59%	0.5033	49.36%	0.3788	48.41%	0.4830
	200	61.46%	0.6138	62.10%	0.6209	55.41%	0.5515	55.41%	0.5535	55.10%	0.5489	52.87%	0.5174	49.04%	0.4864
	500	57.32%	0.5711	57.96%	0.5779	68.79%	0.6837	65.61%	0.6524	61.15%	0.6063	48.73%	0.4858	53.18%	0.5301
	1000	60.83%	0.6065	60.19%	0.5998	79.94%	0.7962	77.07%	0.7673	69.75%	0.6893	58.92%	0.5890	55.73%	0.5573
	2000	69.43%	0.6933	69.11%	0.6904	87.26%	0.8717	83.76%	0.8367	75.48%	0.7517	57.01%	0.5688	57.96%	0.5785
mfeat-factors	50	81.50%	0.7797	76.00%	0.7416	71.00%	0.6668	77.50%	0.7492	73.50%	0.6864	84.00%	0.7908	83.50%	0.8041
	100	91.00%	0.9106	90.00%	0.8993	85.50%	0.8366	86.50%	0.8559	87.00%	0.8618	95.00%	0.9485	92.50%	0.9222
	200	96.00%	0.9587	94.00%	0.9380	91.50%	0.9152	91.50%	0.9147	92.00%	0.9214	96.50%	0.9649	94.00%	0.9399
	500	96.50%	0.9645	95.50%	0.9545	94.50%	0.9451	95.50%	0.9553	93.50%	0.9352	96.00%	0.9587	95.50%	0.9544
	1000	96.50%	0.9645	95.00%	0.9490	95.00%	0.9497	95.50%	0.9550	95.00%	0.9492	97.00%	0.9692	95.50%	0.9537
ozone-level-8hr	50	93.31%	0.6424	95.67%	0.5658	91.34%	0.6711	91.34%	0.6533	95.67%	0.5658	95.28%	0.6544	95.28%	0.6877
	100	92.13%	0.6220	94.49%	0.6357	93.31%	0.6892	92.13%	0.6457	93.70%	0.6199	92.13%	0.6457	93.31%	0.6675
	200	94.09%	0.5899	94.88%	0.5535	91.34%	0.6103	88.19%	0.6107	93.70%	0.6199	95.28%	0.4879	93.70%	0.6199
	500	94.09%	0.6275	95.67%	0.6653	93.31%	0.6675	93.70%	0.6757	94.88%	0.6044	95.67%	0.6222	93.70%	0.6757
	1000	94.49%	0.6357	95.67%	0.6222	90.55%	0.6587	90.94%	0.6273	93.70%	0.6757	94.88%	0.6771	92.52%	0.6921
	2000	94.49%	0.6357	94.88%	0.6044	90.55%	0.6587	90.16%	0.6528	95.67%	0.6222	94.49%	0.5968	93.70%	0.5836
pc4	50	83.56%	0.5788	86.99%	0.5844	79.45%	0.6129	71.92%	0.5943	82.88%	0.5214	73.97%	0.6014	90.41%	0.7045
	100	84.93%	0.6338	86.30%	0.6490	79.45%	0.5655	79.45%	0.6773	85.62%	0.6211	82.19%	0.6067	90.41%	0.4748
	200	86.30%	0.6285	89.73%	0.6719	80.14%	0.6444	78.08%	0.6365	89.04%	0.6622	84.25%	0.6267	92.47%	0.7178
	500	89.73%	0.6939	89.04%	0.6368	84.93%	0.7056	86.99%	0.7304	89.73%	0.6939	90.41%	0.4748	88.36%	0.6932
	1000	93.15%	0.8025	93.15%	0.7542	90.41%	0.7782	89.04%	0.7580	90.41%	0.7235	93.15%	0.7542	91.10%	0.7347

	# train	AML		Fewest misses		XGBoost		LightGBM		Random Forest		SVM		MLP	
		acc.	F_1	acc.	F_1	acc.	F_1	acc.	F_1	acc.	F_1	acc.	F_1	acc.	F_1
philippine	50	66.95%	0.6695	67.98%	0.6798	69.52%	0.6942	68.66%	0.6834	69.01%	0.6896	62.50%	0.6214	67.29%	0.6726
	100	68.66%	0.6852	69.35%	0.6920	69.35%	0.6925	67.29%	0.6716	68.15%	0.6799	67.12%	0.6677	65.41%	0.6540
	200	66.44%	0.6610	67.47%	0.6716	72.26%	0.7224	73.29%	0.7329	69.35%	0.6931	68.66%	0.6854	66.61%	0.6648
	500	67.12%	0.6701	67.12%	0.6688	74.49%	0.7441	72.77%	0.7275	70.21%	0.7005	66.95%	0.6654	63.36%	0.6335
	1000	70.38%	0.7038	70.55%	0.7054	73.12%	0.7312	70.38%	0.7037	71.23%	0.7107	66.78%	0.6665	62.50%	0.6247
	2000	68.32%	0.6830	69.86%	0.6982	74.49%	0.7448	73.97%	0.7397	72.60%	0.7258	66.10%	0.6610	65.41%	0.6536
phoneme	50	76.71%	0.6921	76.52%	0.6858	72.83%	0.6901	78.00%	0.7261	77.45%	0.7114	77.82%	0.7186	77.45%	0.6895
	100	79.30%	0.7289	78.93%	0.7159	81.89%	0.7749	76.89%	0.7324	82.62%	0.7786	78.19%	0.7059	80.22%	0.7177
	200	81.15%	0.7597	80.22%	0.7440	77.45%	0.7454	80.04%	0.7661	81.15%	0.7628	80.41%	0.7640	78.19%	0.7508
	500	83.18%	0.7906	83.73%	0.7954	83.73%	0.8075	83.36%	0.8017	83.18%	0.7923	81.52%	0.7820	81.15%	0.7769
	1000	83.73%	0.7945	84.10%	0.7983	83.55%	0.8070	84.84%	0.8187	82.99%	0.7870	81.70%	0.7838	82.26%	0.7654
	2000	87.06%	0.8392	87.99%	0.8504	87.43%	0.8480	86.69%	0.8397	89.09%	0.8642	84.84%	0.8060	82.99%	0.7980
qsar-biodeg	50	86.79%	0.8484	83.02%	0.7948	81.13%	0.7972	76.42%	0.7478	83.96%	0.8114	74.53%	0.6309	86.79%	0.8484
	100	82.08%	0.8063	83.96%	0.8174	85.85%	0.8453	82.08%	0.8063	83.02%	0.8154	85.85%	0.8453	91.51%	0.9018
	200	86.79%	0.8528	88.68%	0.8720	85.85%	0.8453	83.96%	0.8246	86.79%	0.8528	90.57%	0.8917	94.34%	0.9329
	500	87.74%	0.8582	86.79%	0.8460	87.74%	0.8603	83.96%	0.8224	88.68%	0.8657	90.57%	0.8900	92.45%	0.9120
Satellite	50	99.22%	0.6647	99.41%	0.7842	98.04%	0.6379	98.43%	0.5960	99.02%	0.6404	99.02%	0.7702	99.22%	0.4980
	100	99.22%	0.6647	99.41%	0.6985	98.82%	0.6970	98.82%	0.6220	99.22%	0.6647	99.22%	0.7480	99.22%	0.4980
	200	99.22%	0.6647	99.22%	0.6647	99.22%	0.7480	99.22%	0.7480	99.02%	0.6404	98.82%	0.6220	99.02%	0.4975
	500	99.22%	0.6647	99.41%	0.6985	99.02%	0.6404	98.82%	0.6220	99.02%	0.6404	99.22%	0.6647	99.02%	0.4975
	1000	98.82%	0.6220	99.02%	0.6404	98.82%	0.6220	97.25%	0.6430	99.02%	0.6404	99.02%	0.4975	99.02%	0.6404
	2000	99.22%	0.7480	99.22%	0.7480	99.02%	0.7197	97.45%	0.6112	99.02%	0.6404	99.02%	0.7197	99.22%	0.7480

	# train	AML		Fewest misses		XGBoost		LightGBM		Random Forest		SVM		MLP	
		acc.	F_1	acc.	F_1	acc.	F_1	acc.	F_1	acc.	F_1	acc.	F_1	acc.	F_1
segment	50	76.62%	0.7591	71.00%	0.6959	78.79%	0.7911	80.52%	0.8064	82.25%	0.8275	83.55%	0.8371	77.92%	0.7772
	100	89.18%	0.8956	87.45%	0.8813	87.01%	0.8780	90.91%	0.9155	87.45%	0.8828	88.31%	0.8881	87.45%	0.8788
	200	91.77%	0.9212	90.48%	0.9095	89.18%	0.8970	90.48%	0.9090	91.77%	0.9226	90.48%	0.9108	90.04%	0.9031
	500	95.24%	0.9545	95.67%	0.9592	94.81%	0.9511	93.94%	0.9439	93.51%	0.9378	92.21%	0.9239	94.81%	0.9511
	1000	96.97%	0.9708	96.97%	0.9714	95.24%	0.9550	95.67%	0.9592	94.81%	0.9506	93.94%	0.9417	94.37%	0.9455
	2000	97.40%	0.9749	97.84%	0.9789	97.40%	0.9755	98.27%	0.9835	97.40%	0.9755	95.67%	0.9597	95.24%	0.9565
steel-plates-fault	50	58.97%	0.4691	10.77%	0.0810	57.95%	0.4917	56.41%	0.5092	61.54%	0.6180	60.00%	0.5585	61.03%	0.4653
	100	63.08%	0.6298	62.56%	0.5343	63.59%	0.5936	61.54%	0.6413	70.26%	0.7413	66.67%	0.6909	64.62%	0.6601
	200	73.33%	0.7446	70.77%	0.7460	69.74%	0.7111	67.18%	0.6940	70.77%	0.7430	73.33%	0.7704	70.77%	0.6889
	500	76.92%	0.8119	75.38%	0.7652	75.90%	0.7662	79.49%	0.8316	74.87%	0.8124	72.82%	0.7538	71.79%	0.7344
	1000	81.54%	0.8504	77.44%	0.7919	78.46%	0.8250	77.95%	0.8168	75.38%	0.7658	76.92%	0.7788	71.28%	0.7227
sylvine	50	89.47%	0.8946	89.86%	0.8986	90.84%	0.9084	90.45%	0.9045	88.11%	0.8806	82.46%	0.8240	70.57%	0.6834
	100	87.52%	0.8752	88.89%	0.8888	90.45%	0.9045	88.50%	0.8847	90.25%	0.9024	87.72%	0.8770	83.63%	0.8359
	200	91.03%	0.9103	90.84%	0.9083	91.81%	0.9181	92.40%	0.9240	91.81%	0.9181	88.69%	0.8868	85.96%	0.8596
	500	93.37%	0.9337	92.79%	0.9279	91.81%	0.9181	91.03%	0.9103	92.59%	0.9259	90.25%	0.9025	82.85%	0.8258
	1000	92.79%	0.9279	93.18%	0.9318	93.76%	0.9376	93.76%	0.9376	92.98%	0.9298	90.64%	0.9064	89.47%	0.8944
	2000	93.37%	0.9337	93.76%	0.9376	94.93%	0.9493	95.52%	0.9552	93.18%	0.9318	91.62%	0.9162	89.08%	0.8907
vehicle	50	61.18%	0.5886	60.00%	0.5742	65.88%	0.6376	58.82%	0.5487	64.71%	0.6198	67.06%	0.6573	62.35%	0.5535
	100	65.88%	0.6412	64.71%	0.6255	64.71%	0.6226	63.53%	0.6175	67.06%	0.6338	72.94%	0.7165	71.76%	0.7184
	200	72.94%	0.7211	71.76%	0.7066	75.29%	0.7407	77.65%	0.7609	68.24%	0.6502	65.88%	0.6525	74.12%	0.7290
	500	76.47%	0.7574	74.12%	0.7285	70.59%	0.6792	74.12%	0.7338	74.12%	0.7150	88.24%	0.8773	82.35%	0.8098

	# train	AML		Fewest misses		XGBoost		LightGBM		Random Forest		SVM		MLP	
		acc.	F_1	acc.	F_1	acc.	F_1	acc.	F_1	acc.	F_1	acc.	F_1	acc.	F_1
wilt	50	50.21%	0.3552	92.56%	0.5306	96.28%	0.7535	87.60%	0.5817	95.25%	0.5278	5.17%	0.0495	95.04%	0.4873
	100	89.67%	0.6150	95.25%	0.5278	95.87%	0.7808	95.87%	0.7968	95.87%	0.7511	94.83%	0.7878	95.04%	0.4873
	200	96.28%	0.7946	96.69%	0.7809	94.01%	0.7383	92.15%	0.7149	96.28%	0.7857	98.14%	0.8994	95.45%	0.5652
	500	97.93%	0.8859	98.14%	0.8905	97.52%	0.8735	97.31%	0.8546	96.28%	0.7857	97.93%	0.9019	95.04%	0.4873
	1000	97.93%	0.8859	97.93%	0.8810	97.11%	0.8577	97.93%	0.8946	97.11%	0.8083	97.73%	0.8902	97.93%	0.8810
	2000	97.73%	0.8770	97.93%	0.8810	98.55%	0.9301	98.35%	0.9156	98.76%	0.9315	97.93%	0.9019	98.14%	0.9069
wine-quality-white	50	36.33%	0.2313	34.69%	0.2075	37.76%	0.2780	35.10%	0.2321	41.63%	0.2136	18.16%	0.0599	25.92%	0.1342
	100	39.39%	0.2258	42.24%	0.2151	40.41%	0.2528	33.27%	0.2211	42.65%	0.2321	43.67%	0.1403	45.71%	0.1769
	200	42.86%	0.2507	45.10%	0.2378	40.20%	0.2764	38.16%	0.2605	51.02%	0.2404	44.90%	0.1469	48.16%	0.1640
	500	46.12%	0.2714	47.96%	0.2594	47.55%	0.3372	44.90%	0.4195	50.20%	0.2673	48.98%	0.2277	47.55%	0.2504
	1000	52.45%	0.3384	53.88%	0.3509	51.22%	0.3810	47.35%	0.3491	56.12%	0.3450	52.65%	0.3410	46.53%	0.1691
	2000	57.14%	0.3834	59.18%	0.4091	52.04%	0.3801	53.06%	0.3931	61.02%	0.3950	51.22%	0.2864	52.04%	0.2740
yeast	50	39.60%	0.1924	17.45%	0.1027	36.24%	0.2621	27.52%	0.1985	43.62%	0.3064	40.94%	0.3492	44.97%	0.3105
	100	46.31%	0.3386	47.65%	0.3341	48.99%	0.4651	51.68%	0.4557	54.36%	0.4871	48.99%	0.4255	54.36%	0.3936
	200	44.97%	0.2981	46.31%	0.2906	48.99%	0.3449	44.97%	0.3284	53.02%	0.4189	51.01%	0.4266	46.98%	0.2172
	500	51.68%	0.4794	53.02%	0.4732	54.36%	0.5683	54.36%	0.4592	58.39%	0.4775	51.01%	0.4364	51.01%	0.4995
	1000	54.36%	0.5035	54.36%	0.4820	58.39%	0.5996	57.05%	0.4516	60.40%	0.5878	57.72%	0.5301	53.02%	0.5807